KINETICS STUDY ON BUNSEN REACTION IN A GAS-LIQUID-LIQUID SYSTEM WITH IODINE PROVIDED IN I_2-TOLUENE SOLUTION FOR H_2 FROM H_2S

A Thesis Submitted to the College of

Graduate Studies and Research

In Partial Fulfillment of the Requirements

For the Degree of Master of Science

In the Department of Chemical and Biological Engineering

University of Saskatchewan

Saskatoon

By

JI LI

PERMISSION TO USE

In presenting this thesis in partial fulfillment of the requirements for a postgraduate degree from the University of Saskatchewan, I agree that the libraries of this university may make it freely available for inspection. I further agree that permission for copying of this thesis in any manner, in whole or in part, for scholarly purposes may be granted by the professor or professors who supervised my thesis work or, in their absence, by the Head of the Department or the Dean of the College in which my thesis work was done. It is understood that any copying or publication or use of this thesis or parts thereof for financial gain shall not be allowed without my written permission. It is also understood that due recognition shall be given to me and to the University of Saskatchewan in any scholarly use which may be made of any material in my thesis.

Requests for permission to copy or to make other use of material in this thesis in whole or part should be addressed to:

Head of the Department of Chemical and Biological Engineering

University of Saskatchewan

Saskatoon, Saskatchewan (S7N 5A9)

ABSTRACT

A chemical splitting cycle of H_2S to produce H_2 for sustainable oil sands bitumen upgrading was recently developed

$$H_2SO_4 + H_2S \rightarrow S + SO_2 + 2H_2O$$

$$SO_2 + I_2 + 2H_2O \rightarrow 2HI + H_2SO_4$$

$$2HI \rightarrow H_2 + I_2$$

in which the second reaction, Bunsen reaction, is the link with the other two reactions. With the involvement of organic solvents such as toluene, it is hoped that the reaction will be able to occur without transportation difficulty at room temperature such that side reactions, corrosion and iodine deposition can be effectively mitigated or minimized. The apparent kinetics of the Bunsen reaction is studied in the presence of toluene in a fixed-volume, batch reactor and using the initial rate analysis method. The system includes gas, oil and water phases where reaction and mass transfer coexist. The apparent rate was measured by SO_2 pressure drop vs. time.

In this research project, the effects of SO_2 initial partial pressure from 49.6 kPa to 122.7 kPa and iodine concentration in toluene from 0.045 to 0.235 mol/L on initial reaction rate are reported. The reaction rate is found to be the first order with respect to SO_2 and I_2, respectively. The results of temperature effect show that the reaction followed the Arrhenius equation with an activation energy of 6.02 kJ/mol. The effects of operating conditions on reaction rate including water/toluene volume ratio and stirring speed are also investigated.

The study concludes that the rate-limiting step of the Bunsen reaction in the presence of toluene is the SO_2 dissolving in the liquid phases..

ACKNOWLEDGEMENTS

First and foremost, I am heartily thankful to my supervisor Dr. Hui Wang, for his continuous support and invaluable guidance in my research during last two years. It is his perseverance and enthusiasm that encourage me to finally finish this project.

I also would like to express my deep gratitude to the member of my advisory committee, Dr. Ajay Dalai, Dr. Richard Evitts and Dr. Jit Sharma for their constructive suggestions and encouragements which greatly improve my research.

I also thank students and colleagues I had great pleasure to work with: Mohsen Shakouri, Armin Moniri, Xu Zhao, Yaoya Shen and Lu Tian. I would like to thank Liuqing Yang for her work in solvent screening. I would like to thank Patricia Nuncio for her work in experimental setup.

I wish to thank my mother, Mrs. Zhou Ji, for her tremendous love, support and encouragement.

TABLE OF CONTENTS

LIST OF TABLES

LIST OF FIGURES

NOMENCLATURE

a_{eff}	m^2	Effective interfacial area in rate equation
Aor ABS		Absorbance of ultraviolet–visible spectrophotometer
A_0	m $s^{-1}kPa^{-1}$	Preexponential factor, mol $s^{-1}m^{-2}Pa^{-1}$
C	mol/L	Concentration in Figure 2.5, 4.1
C	mol/L	Constant in Eq.(4.6), (4.7), (4.8) and (4.9)
ε	L $mol^{-1}cm^{-1}$	Molar extinction coefficient,
E_a	kJ/mol	Activation energy
I_0 and I		The intensity of incident light and that of transmitted light, respectively
l	cm	Path length that light will go through
k	m $s^{-1}kPa^{-1}$	Specific reaction rate
k′	mol s^{-1} kPa^{-1}	Regression constant arisen from Eq. (4.5)
k″	L s^{-1}	Regression constant arisen from Eq. (4.6)
m		Order of reaction
n		Order of reaction
n	mol	Number of moles
P	kPa or psi	Pressure
r	mol/s	Initial rate
rpm		Revolutions per minute
R	J $mol^{-1}K^{-1}$	Gas constant
R_P	kPa/s	Initial partial pressure drop rate
t	s	Time
T	K or ^oC	Temperature
UV-Vis		Ultraviolet-visible spectrophotometer
V_W	mL	Volume of water in reaction
V_O	mL	Volume of organic (toluene in this study) in reaction
[ ]	mol/L	Molarity

CHAPTER 1

INTRODUCTION

1.1 H_2S splitting cycle

The efforts of converting hydrogen sulfide from gas and oil industries into hydrogen are always beneficial economically. In petroleum industry, especially bitumen and heavy oil upgrading and refining process, vast amount of hydrogen is required and H_2S is produced. H_2S is then turned into elemental sulfur such as the Claus plant (Gamson et al., 1953), and the water is disposed into the environment. The hydrogen used here is mainly produced by steam reforming of natural gas. This process not only consumes clean fossil fuels but also releases greenhouse gas CO_2. Furthermore, hydrogen produced by this way finally goes into water and is difficult to recycle. In view of the adverse effect as mentioned above, a novel hydrogen production by H_2S splitting cycle was proposed for the first time by Wang, (2007). It contains reactions (1.1), (1.2) and (1.3) as follows:

$$H_2SO_4 + H_2S \rightarrow S + SO_2 + 2H_2O \quad (1.1)$$

$$SO_2 + I_2 + 2H_2O \rightarrow 2HI + H_2SO_4 \quad (1.2)$$

$$2HI \rightarrow H_2 + I_2 \quad (1.3)$$

The overall reaction is:

$$H_2S \rightarrow H_2 + S \quad (1.4)$$

This new H_2S splitting cycle allows the conversion of H_2S into H_2 and elemental S with two working reagents I_2 and H_2SO_4 recycled. Furthermore, if the sulfur produced by reaction (1) is continued to be oxidized into SO_2 by reaction (1.5), reactions (1.2) and (1.3) would occur in a double scale because two moles of SO_2 are produced. As a result, the overall reaction becomes reaction (1.6) instead of (1.4). In this way, the modified cycle called H_2S-H_2O splitting cycle was further proposed:

$$H_2SO_4 + H_2S \rightarrow S + SO_2 + 2H_2O \quad (1.1)$$

$$S + O_2 \rightarrow SO_2 \quad (1.5)$$

$$2SO_2 + 2I_2 + 4H_2O \rightarrow 4HI + 2H_2SO_4 \quad (1.2)$$

$$2HI \rightarrow H_2 + I_2 \quad (1.3)$$

The overall reaction is

$$H_2S + 2H_2O + O_2 \rightarrow 2H_2 + H_2SO_4 \quad (1.6)$$

This new cycle produces two moles of hydrogen and one mole of sulfuric acid from one mole of H_2S. Both H_2S and H_2S-H_2O splitting cycles are sustainable processes to facilitate a sustainable upgrading process of oil sands without CO_2 emission. The engineering objective of both cycles is to develop processes carrying out all of the above reactions and related separations.

H_2S or H_2S-H_2O splitting cycle is based on two reaction system, one is the gas-liquid reaction system of H_2S and H_2SO_4 (reaction 1), which has been studied by Zhang et al. (2000) and Wang et al. (2002a; 2002b; 2003). The other is the well-known

thermochemical sulfur-iodine (S-I) water splitting cycle (Brown et al., 2000; 2002) shown as follows:

$$H_2SO_4 \rightarrow 0.5O_2 + SO_2 + H_2O \quad (1.7)$$

$$SO_2 + I_2 + 2H_2O \rightarrow 2HI + H_2SO_4 \quad (1.2)$$

$$2HI \rightarrow H_2 + I_2 \quad (1.3)$$

The overall reaction is

$$H_2O \rightarrow H_2 + 0.5O_2 \quad (1.8)$$

Sulfuric acid is decomposed at high temperature (800-900 ^oC) (reaction 1.7). The S-I cycle has been considered the one of the most promising routes for hydrogen production in large scale (Goldstein et al., 2005; Vitart et al., 2006).

Since the only difference between S-I water splitting cycle and the H_2S splitting cycle is reactions (1.1) and (1.7), the research progresses achieved in the former system can be applied to the latter. The current research on S-I water splitting cycle indicates that the Bunsen reaction is the key reaction to determine the overall efficiency, because its products, mixture of H_2SO_4 and HI, have to be purified to feed reactions (1.7) and (1.3), and this purification process is the most energy consuming step (Brown et al., 2000; 2002). This situation is the same for H_2S or H_2S-H_2O splitting cycle. Therefore, in order to optimize the H_2S or H_2S-H_2O splitting cycle, it is important to develop an efficient way to carry out the Bunsen reaction. A literature review about the current routes of operating the Bunsen reaction will be given in Chapter 2.

1.2 Organization of this thesis

In this thesis, Chapter 1 introduces the background of H_2S splitting cycle. Chapter 2 is a literature review on the studies of Bunsen reaction and gas-liquid-liquid reaction system. Following the review, the knowledge gap and research objectives of this project are included in this part. Chapter 3 describes the experimental methods, including the specific experimental procedures, analytical methods of various components in the system and calculations of reaction rates in the closed gas-liquid reactor. Chapter 4 presents the results and discussion. Chapter 5 draws the conclusions made from the discussion and future work.

CHAPTER 2

LITERATURE REVIEW

The Bunsen reaction has been widely studied in the S-I water splitting cycle, which is the key step to decide on the efficiency of both cycles: S-I water splitting cycle and H_2S splitting cycle. A review on the research background of Bunsen reaction and gas-liquid-liquid reaction system is discussed in this chapter.

2.1 General Atomic stoichiometry of Bunsen reaction in S-I cycle

2.1.1 Operation and application

The operation of General Atomic stoichiometry on the Bunsen reaction was proposed by General Atomics (Norman et al., 1981) in the study of the S-I water splitting cycle. This method is to operate the Bunsen reaction in a large excess of iodine in the liquid water media to separate the two products acids into two immiscible liquid phases: a Heavier HIx phase and a lighter sulfuric acid phase. The heavier HIx phase consists of hydrogen iodide, iodine and water, where the lighter phase is the diluted sulfuric acid, described by the following equation (Giaconia et al., 2007):

$$\begin{aligned} &SO_2 + 16H_2O + 9I_2 \rightarrow \\ &(2HI + 10H_2O + 8I_2)_{\text{HIx phase}} + (H_2SO_4 + 4H_2O)_{\text{Sulfuric acid phase}} \end{aligned} \tag{2.1}$$

The temperature of reaction (2.1) is 120 ^{o}C to maintain the I_2 in liquid state since the melting point of I_2 is 113.7 ^{o}C. A demonstration process for Reaction (2.1) combined with

reaction (1.3) built in Japan was able to produce H_2 at rate of 50 L/h for 33 hours (Mizuta et al., 1990). Yields of the constituent reactions, and the amount of water used in the cycle, thermal efficiency of the whole Mg-S-I cycle was evaluated to be 17-39 % as a function of the overall heat recovery (65-85 %).

The General Atomic method was widely studied as a part of the S-I cycle. Some of researchers focused on the separation and purification of sulfuric acid and HIx phases. The purification process was investigated by Zhang et al., (2010) in a continuous mode by reacting sulfuric acid and HI in a packed column. In this study, the influences of operational parameters were evaluated including the reaction temperature, the flow rate of nitrogen and the raw material solutions, on the purification efficiency. The suitable conditions for continuous purification process of the two phases were proposed also by Guo et al., (2010).

2.1.2 Problems in operation

Although the method based on the GA stoichiometry allows physical separation between HI and H_2SO_4, it leads to more other problems in operation. Intensive energy was required to extract and recycle prior to the decomposition subunits. Moreover, sulfuric acid phase contains only 57 (wt)% H_2SO_4 and needs to be concentrated. The molar ratio of HI to H_2O is 1:5 in HIx phase, which is very close to the ratio of azeotrope of HI and H_2O (1:5.36) at atmospheric pressure. H_3PO_4 (O'Keefe et al., 1982)

and reactive distillation (Roth et al., 1989) were used for the extractive distillation, which were believed to be the most expensive and energy intensive consumption steps.

Furthermore, this method is to run the Bunsen reaction at 120 ^{o}C, slightly above the melting point of iodine (113.7 ^{o}C) at atmospheric pressure, which leads to the iodine vapor deposition everywhere in the setup that may block the tubes, and also causes severe corrosion due to H_2SO_4 and HI/I_2 solutions. Large amounts of I_2 and water circulated in the system, and as a result, water removal becomes a critical concern.

2.1.3 Side reactions

At 120 ^{o}C at which the Bunsen reaction is run , the following two side reactions are feasible during the Bunsen reaction, which consume the formed HI and H_2SO_4 (Sakurai et al., 2000):

$$6HI+H_2SO_4 \rightleftharpoons S+ 3I_2 +4H_2O \quad (2.2)$$

$$8HI+H_2SO_4 \rightleftharpoons H_2S+ 4I_2 +4H_2O \quad (2.3)$$

The concentration of HI, H_2SO_4 and I_2 solutions and temperature conditions were studied under which those side reactions occur: reaction (2.3) is favored between 20 ^{o}C and 95 ^{o}C over reaction (2.2), the opposite under low iodine excess. Both equations are enhanced by a higher acid concentrations and higher temperatures.

2.2 Survey of the Bunsen reaction routes to improve its energy efficiency

Besides the General Atomic, abundant relevant researches on the Bunsen reaction were devoted to reduce the consumption of I_2 and H_2O and therefore decrease the energy burden caused. Recent progresses of the Bunsen reaction operations are reviewed below.

2.2.1 The Bunsen reaction with a precipitation agent

Metathesis reactions with formation of insoluble solid salts lead to liquid-solid separation instead of original liquid-liquid separation of hydroiodic acid and sulfuric acid (Sau et al., 2008). For example, lead sulphate was used in this method as shown in Figure 2.1. The accompanying reactions are:

$$PbSO_4(s) + 2HI(aq) \rightarrow PbI_2(s)\downarrow + H_2SO_4(aq) \quad (20\text{-}120\ ^oC) \tag{2.4}$$

$$PbI_2(s) + 2HPO_3(aq) \rightarrow 2HI(g) + Pb(PO_3)_2 \quad (420\text{-}450\ ^oC) \tag{2.5}$$

$$Pb(PO_3)_2 + H_2SO_4 + 2H_2O \rightarrow PbSO_4(s) + 2H_3PO_4(aq) \quad (20\text{-}80\ ^oC) \tag{2.6}$$

Reaction (2.5) and (2.6) regenerate $PbSO_4$ and recycle it to the process. This route strongly decreases the recirculation rate of recycling agents (iodine and water) and avoids energy-intensive HIx process, but it has the disadvantage of adding solid material and concentrated phosphoric acid management.

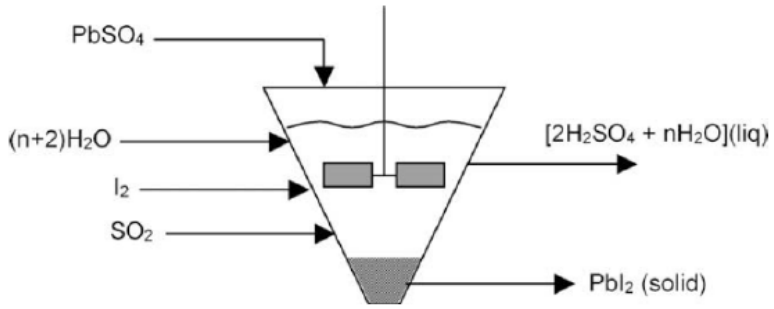

Figure 2.1 Scheme of the Bunsen reaction with insoluble lead sulphate (Giaconia et al., 2009)

2.2.2 The Bunsen reaction in organic solvents

The Bunsen reaction in organic solvents was first discussed by De Beni et al., (1980). Organic solvents were involved into the system to dissolve reactants I_2, SO_2 and H_2O, and the product HI. Thus, HI stays in organic phase and so is separated from H_2SO_4 which stays in the water phase. For example, tributyphosphate (TBP) was selected for the Bunsen reaction due to its good solubility for SO_2. The resulting TBP and SO_2 mixture can dissolve a smaller but sufficient amount of I_2 and H_2O for the Bunsen reaction. The process is illustrated simplified in Figure 2.2, where the product H_2SO_4 and HI were separated by staying in the different phases. This method greatly reduced the excess amount of iodine, but the most difficult part was the HI recovery from the organic solvent.

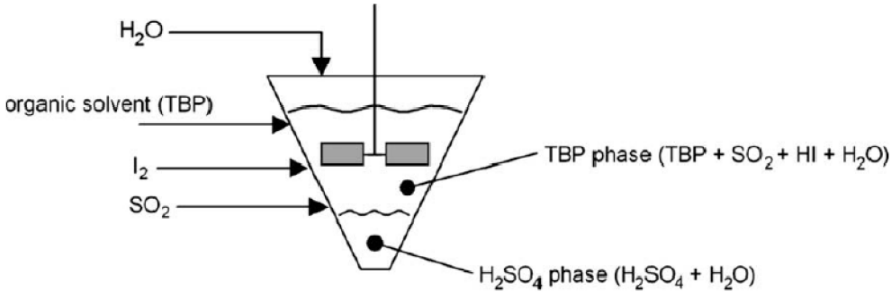

Figure 2.2 Scheme of the Bunsen reaction in TBP (Giaconia et al., 2009)

2.2.3 The Bunsen reaction in an electrochemical membrane reactor

The application of electrochemical membrane reactor (Figure 2.3) to run the Bunsen reaction was proposed by Nomura et al., (2004a, 2004b).

$$\text{Anode side reaction: } SO_2 + 2H_2O \rightarrow H_2SO_4 + 2H^+ + 2e^- \quad (2.7)$$

$$\text{Cathode side reaction: } I_2 + 2H^+ + 2e^- \rightarrow 2HI \quad (2.8)$$

In this method, two acids are physically separated by the electrochemical membrane reactor and the excess use of iodine is effectively avoided. However, the products are two diluted acids for large amount of water is required for the permeation of proton through the exchange membrane (Figure 2.3). Thus, this method still needs more improvement.

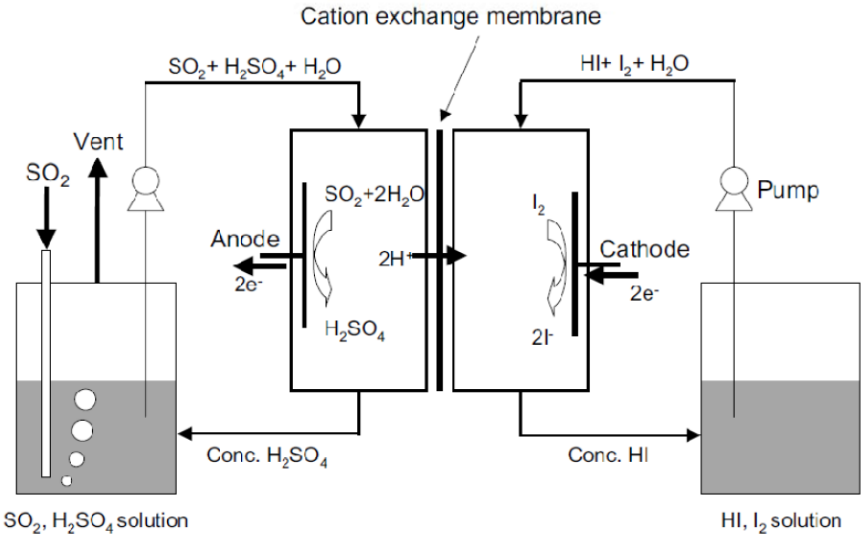

Figure 2.3 Scheme of an electrochemical membrane reactor (Nomura et al., 2004[a])

2.3 The proposal of the Bunsen reaction in the presence of organic solvents

From the literature above, it can be noted that one big challenge for the operation of the Bunsen reaction is to substantially reduce the excess use of I_2 and H_2O. Moreover, it is also a challenge to lower the reaction temperature and facilitate the purification of HI and H_2SO_4 aqueous mixture. Wang (2008) proposed a new method of carrying out the Bunsen reaction in organic solvents. The idea is to use organic solvents to dissolve the solid iodine. Toluene and water (excess amount) are fed into a reactor, a two-phase reaction mixture is formed. Once the gaseous SO_2 is introduced into water phase, the Bunsen reaction is initiated. Figure 2.4 illustrates this suggestion. During the reaction, the reactant iodine has much higher solubility in toluene than in water and easily

moves to water phase to supply the Bunsen reaction; the HI and H_2SO_4 will stay preferentially in water phase. As a result, the Bunsen reaction does not have to occur at 120 ^oC for melting solid iodine and the use of iodine and water is greatly reduced. The reaction can be operated at room temperature, so that the vapor pressure of I_2 is low and thus, the I_2 deposition becomes negligible. Moreover, HI should not dissolve in the organic solvent, and HI/I_2 solution should not form so that the corrosion problem is eased.

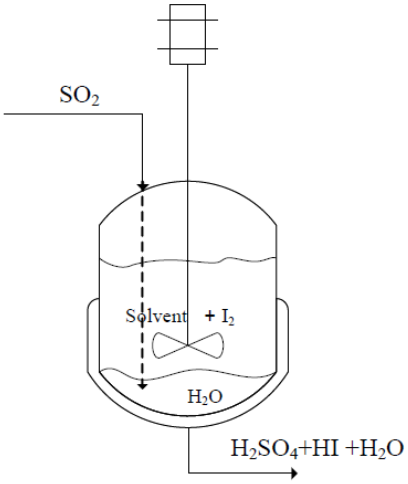

Figure 2.4 Schematic diagram of the Bunsen reaction in the presence of organic solvents

2.4 The selection of organic solvents suitable for the Bunsen reaction

The purpose of the introduction of organic solvents in the Bunsen reaction is to dissolve the solid iodine to make it in fluid below it melting point. Therefore, the organic solvents with higher solubility for iodine should be reviewed. Hildebrand et al.

(1950) studied the iodine solubility in the ordinary organic solvents, from which the suitable organic solvents for the Bunsen reaction was screened out by Yang (2010) as Table 2.1 shows.

Table 2.1 Screening of organic solvents for the Bunsen reaction
reproduced from Yang (2010)

Organic solvents	Iodine Solubility, g/mL,25^{o}C	Boiling point^{o}C	H/F/R*	Density g/mL	Solubility in water (g/100mL,20^{o}C)
Benzene	0.146	80	2/3/0	0.88	0.08
Toluene	0.163	110	2/3/0	0.87	0.05
o-xylene	0.180	144	2/3/0	0.88	insoluble
p-xylene	0.169	138	2/3/0	0.86	insoluble
m-xylene	0.185	139	2/3/0	0.86	insoluble
1,2,3-trimethylbenzene	0.208	175	0/2/0	0.89	0.005
1,2,4-trimethylbenzene	0.187	169	1/2/0	0.88	very poor
1,3,5-trimethylbenzene	0.216	165	2/2/0	0.86	very poor
1,2,3,4-tetramethylbenzene	0.226	205	1/2/1	0.90	insoluble
ethylbenzene	0.129	136	2/3/0	0.87	0.015
n-butylbenzene	0.114	159	0/2/0	0.86	slightly
cumene	0.108	152	2/3/0	0.86	insoluble
n-butylbenzene	0.094	183	0/2/0	0.86	insoluble
isobutylbenzene	0.081	170	2/2/0	0.85	insoluble
tert-butylbenzene	0.086	169	2/3/2	0.87	insoluble
chlorobenzene	0.086	132	1/3/0	1.11	low
bromobenzene	0.140	156	1/2/0	1.49	insoluble
n-C6H14	0.009	69	1/3/0	0.65	0.0013
n-C7H16	0.012	98	1/3/0	0.68	immiscible
CCL4	0.030	76	3/0/0	1.59	0.08
CHCl3	0.074	61	2/0/0	1.48	0.8
CS2	0.243	46	3/4/0	1.26	0.29
cyclohexane	0.022	81	1/3/0	0.78	immiscible
ethyl alcohol	0.215	78	1/3/0	0.78	miscible
ethyl ether	0.240	35	2/4/1	0.71	6.9

*H: Level of health hazard; F: level of flammability; R: level of reactivity

Although ethyl ether and ethyl alcohol have higher solubility for iodine, ethyl ether is very volatile and highly flammable and ethyl alcohol is miscible in water. The aromatic solvents such as toluene, xylene, trimethylbenzene, chlorobenzene and bromobenzene may be suitable for the Bunsen reaction. These water-insoluble compounds have low volatility and good chemical inertia. Initially in our lab, Le Person (2008) chose toluene as the solvent for the Bunsen reaction. Toluene is a water-insoluble aromatic solvent with boiling point at 110 ^{o}C and low toxicity, thus suitable for the Bunsen reaction. Also, there is no reaction between toluene and iodine by the NMR results obtained by Yang.

2.5 Iodine solubility in water and the dissolving effect of HI on the solubility

The Bunsen reaction is proposed to run in the presence of organic solvents, which is a combination of an organic solvent, iodine, water, HI and H_2SO_4. Iodine solubility in pure water is very small (0.3404 g/L). However, the existence of iodide and proton will greatly increase the iodine solubility in water. One reason is that iodine crystals can dissolve rapidly in an iodide aqueous solution by forming soluble triiodide ions (I_3^-). The other reason is that polyiodine species, I_{2X}, where X=1, 2, 3 etc., will be stabilized by H^+ in the solution (calabrese et al., 2000). Iodine solubility in the concentrated hydroiodic acid solution (45.9-66.7 wt % HI) was summarized in Table 2.2 (Adapted from Powell et al., 1947)

Table 2.2 Iodine solubility in concentrated hydroiodic acid

HI, wt %	Gravity,25 ^{o}C	I_2,kg/L	I_2,kg/kg	I_2,mol/HI,mol
66.7	1.95	5.22	2.68	2.03
64.0	1.88	4.72	2.52	1.98
54.4	1.64	3.47	2.11	1.95
50.2	1.56	2.84	1.82	1.83
45.9	1.49	2.28	1.85	1.68

2.6 Mechanism and kinetics of Gas-liquid-liquid reaction

With the involvement of the organic solvent such as toluene in the Bunsen reaction, a gas–liquid–liquid system of gaseous phase, aqueous phase and organic phase is encountered. The kinetics of such processes tends to be complex, for most practical cases, there is no way to determine mass transfer rates and chemical reaction rates separately. The gas-liquid mass transfer and reaction, liquid-liquid mass transfer and reaction may influence the kinetics of reaction. The two-film model is always used to describe the mass transfer and the reactions in either gas or liquid phase.

2.6.1 Two-film model

The two-film model, originally proposed by Lewis and Whitman (1924), is a simplified model used to describe mass transfer at the gas-liquid interface (Figure 2.5).

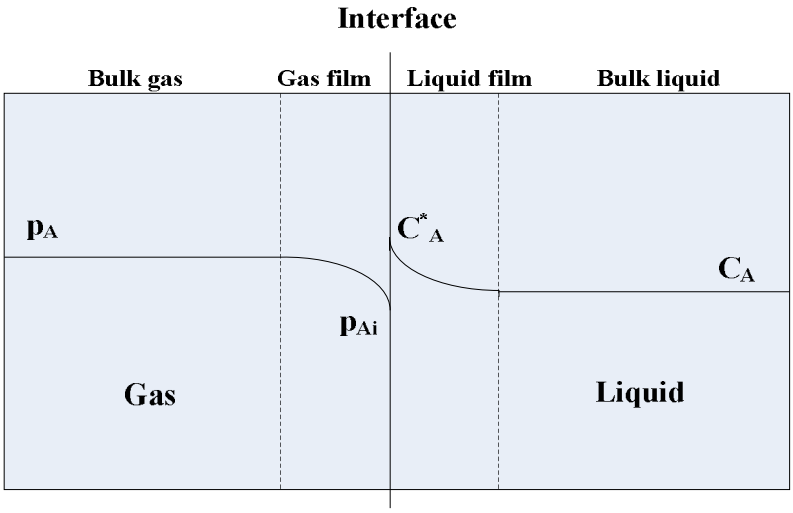

Figure 2.5 Schematic of the two-film model adapted from Danckwerts (1970)

It is assumed that the gas and the liquid are in equilibrium at the interface and that the thin films separate the interface from the bulk of both contacting phases. Furthermore, transfer occurs within these films by molecular diffusion alone. Outside the films, in the bulk fluid phase, the level of turbulence is so high that there is no composition gradient at all. Also, there is no gradient in the bulk gas phase.

2.6.2 Rate-limiting step identification

It is difficult to deduce the kinetic equation from the analysis of mass transfer and the reaction due to the complexity of the gas-liquid-liquid reactive process (Lu et al., 2011). However, in many cases, the process rate is controlled by one or several rate-limiting steps. If the rate-limiting step could be identified, the kinetic equation can be simplified. In multiphase systems, either gas-liquid-solid or gas-liquid-liquid,

frequently the absorption rate of a soluble gas phase reactant is the rate-limiting step (Beenacher et al,. 1993; Poncin et al., 2002) for the overall process. Some relevant discussion below can be used to deduce the rate-limiting step.

Chemical reaction are often classified as “fast” or “slow” perhaps with a vague category of “moderately fast” in between. In general, either of the three cases can exist (Danckwerts, 1970; Kaur et al. 2007): (1) When diffusion is slow by order of magnitude in comparison to chemical reaction, the mass transfer between reaction species, or in other words, diffusion of the reaction gas into bulk liquid phase (in gas-liquid reaction) controls the reaction rate. Thus, if the reaction is fast, the bulk flow properties can have a significant effect on the reaction rate. By inducing bulk movement, for example, by increasing the degree of agitation, the mass transfer increases, thus there is a corresponding increase in the rate of reaction. (2) If the chemical reaction is slow as compared to the rate of diffusion, bulk movements by means of increasing the degree of agitation have no effect on the reaction rate. In this case, the chemical reaction is the only rate-limiting step. (3) If the mass transfer and chemical reaction are of same order of magnitude, the bulk movements induced by agitation, can play a significant role in increasing the reaction rate, but it is not the sole criteria for rate-limiting step identification. This type of reactions comes under the category of “moderately fast” reactions. Besides, the process rate would be very sensitive to temperature by reaction control than by mass transfer control (Hu et al., 2002).

2.7 Knowledge gap

According to above literature review and the proposal of the Bunsen reaction in the presence of organic solvents, the knowledge gaps are concluded as follows:

1. Up to date, neither General Atomic stoichiometry nor other new methods are available to run the Bunsen reaction in an efficient way.
2. One of new attempts to explore the Bunsen reaction is to run the reaction in the presence of organic solvents. The suitable organic solvents have been screened and toluene was chosen initially, but there is not any kinetic study of the Bunsen reaction in the presence of toluene in a closed batch reactor.
3. The impact of reaction condition including phase ratio of water and toluene used in the system and agitation speed has not been reported.
4. The kinetics of Bunsen reaction in the presence of toluene based on multiphase reactions has not been systematically studied yet.
5. There is not any effective method to separate the main products: H_2SO_4 and HI.

2.8 Research objectives

The goal of this project is to study the Bunsen reaction systematically in the presence of toluene in a batch reactor. The research objectives can be described as follows:

1. Evaluate the effects of the operating conditions, such as water/toluene volume ratio and agitation speed on the reaction rate.
2. Investigate the kinetics based on gas-liquid-liquid reaction system to have further understanding about reaction rate equation establishment and activation energy of Bunsen reaction, which has been prescribed as one of the primary goals of this project.
3. Identification of the rate-limiting step.

CHAPTER 3

EXPERIMENTAL METHODS

3.1 Chemicals

All chemicals used for experiments are ACS grade as received without further purification: Iodine (>99.9 %) supplied by Acros Organics, sulfur dioxide (>99.9 %), sodium hydroxide (EMD), sodium thiosulfate anhydrous (Fisher), sodium iodide (BDH), and toluene (BDH). Sulfuric acid (96 wt%) (Fisher). All solutions were prepared by dilution with deionized water.

3.2 Experimental setup

The setup used for experimentation is as shown in Figure 3.1. The reactor used in this experiment is a series compact mini-reactor with a 300 mL volume and made of 316 stainless steel (Model 5500, Parr Instrument Co, USA), equipped with a magnetic stirred drive and a glass liner inside the reactor. The glass liner with a 5.7 cm inner diameter, was used to prevent the stainless steel parts of the reactor from contacting the corrosive solutions such as iodine in toluene, sulfuric acid and hydroiodic acid produced. The reactor was equipped with a block heater which was connected to the reactor controller (Model 4848, Parr Instrument Co, USA). The agitation speed could also be controlled by the reactor controller. The pressure of the system was measured by the pressure

transducer (Scadasense 4102, Control Microsystems), which has a 0.1 psi resolution. The temperature of the reactor was monitored by the reactor controller, read to 0.1 ^{o}C. A two-stage vacuum pump (Model 15601, Robinair Co, USA) was used to remove the air inside the setup. Two rotameters (which were calibrated in advance) were used to measure the flowrate of N_2 and SO_2 going in and coming out from the reactor respectively.

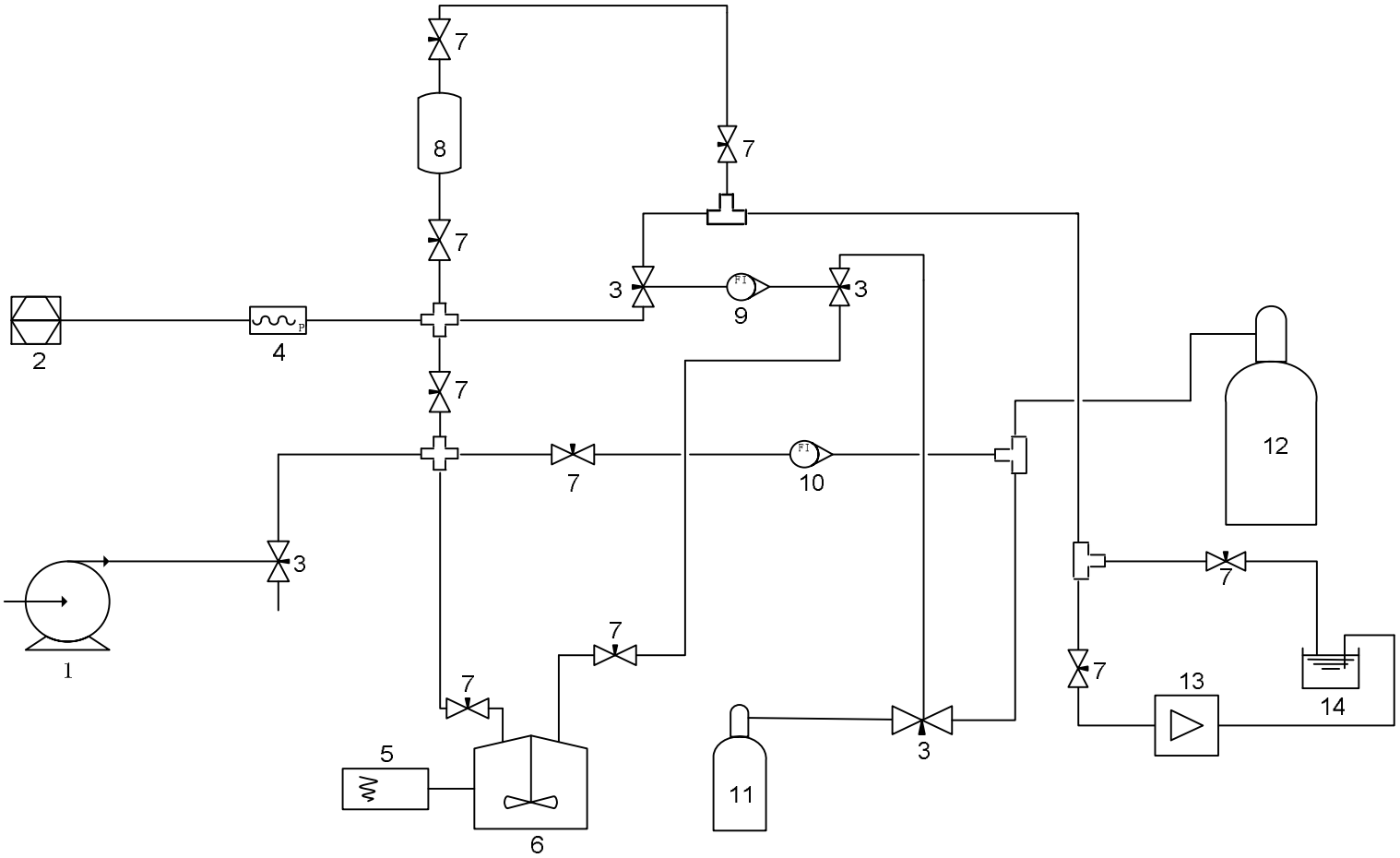

Figure 3.1 Schematic diagram of experimental setup for Bunsen reaction: (1) Pump; (2) Computer; (3) three-way valve; (4) Pressure transducer; (5) Reactor controller; (6) Series compact reactor; (7) two-way valve; (8) SO_2 reservoir; (9)rotameter for N_2; (10) rotameter for SO_2; (11) SO_2 cylinder; (12) N_2 cylinder; (13) Gas Chromatograph (14) NaOH absorber

3.3 Experimental procedure

3.3.1 General experimental procedure

No matter what the conditions at which the experiments were run, the procedure of a general run is described as follows:

1. Connect the reactor to the feed part of the experiment setup and vacuum the system. Fill the system with 10 psi nitrogen and vacuum it again, repeat several times to take the impurities of gas out of the system.
2. Fill the system with nitrogen to 30 psi to check leakage. If the pressure drop is less than 0.1 psi in one hour, the system is considered to have no leakage.
3. Leave 5-10 psig nitrogen, open the cap in the top of the reactor. Keep 100-200 mL/min flowrate of nitrogen filled into the system.
4. Inject a certain concentration of iodine in toluene solution and some volume of water into the reactor respectively by Teflon tube (1/8 inch) and syringe.
5. Afterwards, cap the system and leave 2 psig nitrogen in the system.
6. Heat the system to certain temperature if needed.
7. After the temperature reached equilibrium, fill the pure SO_2 from the cylinder to the reservoir firstly to a certain pressure and record it.
8. After controlling the agitation speed to 100 rpm or 200 rpm, the system is ready for the reaction. Then introduce pure SO_2 from the reservoir into the reactor, take this moment as time zero. Record this pressure, denoted as P_1. Once SO_2 has been

introduced into the reactor, record the pressure of the gas phase P, every second using the pressure transducer. This step is done automatically by a computer connected to the pressure transducer.

9. Obtain the initial partial pressure drop rate, R_P, in terms of the slope at t=0 of the curve of ΔP, or $P - P_1$, versus time. Then convert ΔP to ΔN_{SO_2} with $PV = nRT$, where the volume of the system was measured in advance. Then the SO_2 consumption, ΔN_{SO_2}, versus time t was plotted, as shown in Figure 3.2. Then the function was obtained in terms of $\Delta N_{SO_2} = f(t)$ for the time range of 0 to 100 s. The initial rate, r was obtained from the differential result of the function at t=0, that is $r = f'(0)$, which is the slope of the curve at t=0. The specific calculation for ΔN_{SO_2} and r are reported later in Section 3.5.
10. Run the reaction for one or two hours, then the system was purged with nitrogen for about half an hour to remove any SO_2 unreacted. The final gas in the reactor was analyzed using Varian CP3800 gas chromatograph (GC) equipped with pulsed flame photometric detector (PFPD) if needed. The liquid phase after reaction would be analyzed after dilution.

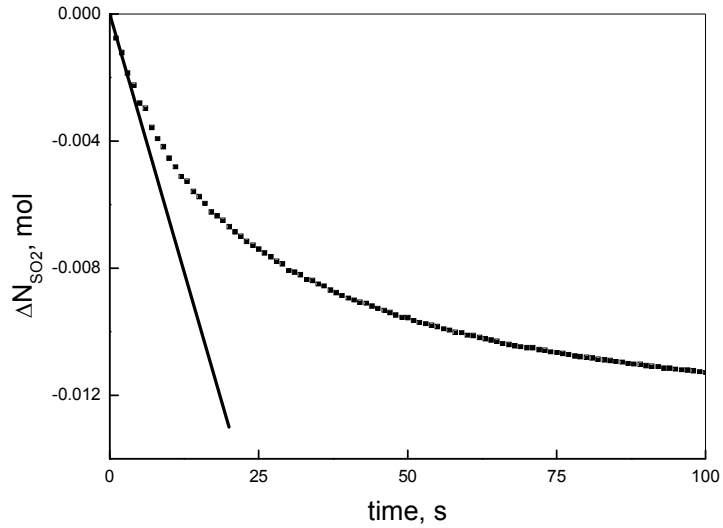

Figure 3.2 Plots of SO_2 consumption vs. time for Bunsen reaction:
the slope at time zero gives the initial reaction rate

3.3.2 Specific conditions for each group of runs

The experiments were run at room temperatures (22 ^{o}C) unless indicated. The experiments were run at 32, 42 and 52 ^{o}C respectively to study the effect of temperature on initial reaction rate. The temperatures of the gas and the liquid in the closed reactor should be the same and constant even though this may difficult to realize. In this study, the temperature of the liquid was heated and controlled by the reactor controller. The gas phase was not heated directly and therefore, was assumed to be at room temperature when the moles of gas were calculated by the equation of state for an ideal gas. In fact, as the temperature of the gas and liquid differed, the warmer liquid would heat the gas close to the liquid, leading to a temperature gradient in the gas phase (Wang et al., 2002).

However, the error thus introduced to the calculation of total moles of SO_2 would not significant because, firstly, SO_2 at room temperature was introduced into the reactor just before the reaction started, secondly, the gas phase was at room temperature initially and only the gas close to the liquid would be heated and reacted, most importantly, the temperature difference between the gas (22 ^oC) and the liquid (maximum 52 ^oC) was not large.

The conditions for the experiments are including agitation speed, volume phase ratio of water to toluene, iodine concentration in toluene, SO_2 initial partial pressure and temperature. The agitation speed was usually set to 100 rpm or 200 rpm, phase ratio was set to 0.7:80 unless indicated. The specific conditions as above for each group are reported in Chapter 4 accordingly.

3.4 Analytical methods

As mentioned earlier, the composition of the liquid phases after reaction runs was analyzed. The corresponding analytical methods for various components in the liquid phase were as followings:

The proton concentration in water phase was determined by titration with a standard 0.5 mol/L sodium hydroxide solution using phenolphthalein as the indicator. The iodine concentration in water phase was determined by titration with a standard 0.1 mol/L sodium thiosulfate using thyodene as the indicator. The iodine concentration in

toluene phase and the iodide ion concentration in the water phase were determined by UV mini 1240 UV-Vis spectrophotometer from Shimadzu and Mandel 10 mm path length quartz cuvettes (see details in Appendix A).

3.5 Calculation of the initial rate

Take the run for 0.146 mol/L iodine concentration, 100 rpm, 0.35:80 phase ratio and 22 ^{o}C as an example. ΔN_{SO_2} was calculated from ΔP by

$$\Delta N_{SO_2} = \frac{\Delta P \cdot V}{RT} \tag{3.1}$$

where, V is the volume of gas phase, which is 0.000308 m^3, R is 8.314 Pa $m^3K^{-1}mol^{-1}$, T is the absolute temperature in K. Then ΔN_{SO_2} corresponding to ΔP between any time and the initial time in the unit of second can be calculated, then the plot of the SO_2 consumption against time was plotted by the software Origin 7.5 in Figure 3.2. Then several regressions were fit to the curve for the range of 0 to 100s, the second order exponential decay regression was the best fit ($R^2 > 0.999$). Then the function was obtained in terms of $\Delta N_{SO_2} = f(t)$, as Eq. (3.2) shows.

$$\Delta N_{SO_2} = f(t) = \mathrm{A} * \exp(-t/a) + \mathrm{B} * \exp(-t/b) - \mathrm{C} \tag{3.2}$$

A= 0.00336 ± 0.00003 a= 7.24 ± 0.19

B= 0.00450 ± 0.00006 b= 41.99 ± 1.22

C= 0.00790 ± 0.00003

R^2= 0.9997

Then, the initial rate, r was obtained from the differential result of the function at t=0, that is $r = f'(t = 0) = 5.7 \times 10^{-4} mol / s$.

CHAPTER 4

RESULTS AND DISCUSSION

4.1 Mechanism aspect of Bunsen reaction in the presence of toluene

With the involvement of organic solvent such as toluene in the Bunsen reaction, a gas–liquid–liquid reaction is encountered where there are one gas phase and two immiscible liquid phases, the aqueous phase and organic phase. However, our understanding of the gas-liquid–liquid reaction system is not well developed today despite their widespread use in the process industries. The Bunsen reaction in the presence of toluene would lead to very complicated mechanism. Without toluene in the system, the Bunsen reaction can be translated into two steps:

$$SO_2(g) + H_2O(l) \rightleftharpoons H^+(aq) + HSO_3^-(aq) \quad (4.1)$$

$$H^+(aq) + HSO_3^-(aq) + I_2(l) + H_2O(l) \rightleftharpoons H_2SO_4(aq) + 2HI(aq) \quad (4.2)$$

Although it has not been discussed in publications, the `two-step mechanism can be supported by the following arguments. (1) SO_2 is a stable gas and its reducing ability is small. The study in the Claus reaction has shown that gas SO_2 and H_2S will not react at any temperature unless there is involvement of a catalyst or liquid medium (Gamson et al., 1953). (2) The experiment involving only I_2 and SO_2 shows no reaction. Iodine consumption was not observed after passing SO_2 gas through the I_2-toluene solution (Le Person, 2008). (3) SO_2 is soluble in water, and the dissolution results in the formation of

sulfurous acid solution or hydrogen bisulfite solution, which has stronger reducing ability (Jolly, 1991). The Gibbs free energy calculation also indicates that the two-step is more thermodynamically favorable. Table 4.1 and 4.2 shows the results of $\Delta H, \Delta S, \Delta G$ and K of reaction 4.2 and Bunsen reaction (1.2), respectively, calculated by HSC software for the temperature range of the interest of this investigation. The results indicate that the Bunsen reaction can not occur without ionizing the products ($\Delta G>0$ at 22-52 ^{o}C). It can be seen that water plays not only the role of a solvent for SO_2 to form more reducible bisulfate anion but also the role to ionizing the products, HI and H_2SO_4, such that the thermodynamics favors the reaction to proceed to the right-hand side. This discussion also confirms that the reaction must take place in the aqueous phase where the I_2 molecules and bisulfate anions contact.

Table 4.1 $\Delta H, \Delta S, \Delta G$ and K of reaction (4.2) calculated by HSC

$$HSO_3^-(aq) + H^+(aq) + I_2(l) + H_2O(l) = 4H^+(aq) + 2I^-(aq) + SO_4^{2-}(aq)$$

T, °C	△H, kJ	△S, J/K	△G, kJ	K	Log(K)
22	-136.3	-237.5	-66.2	5.2×10^{11}	11.7
32	-142.7	-258.9	-63.7	8.0×10^{10}	10.9
42	-148.8	-278.4	-61.0	1.3×10^{10}	10.1
52	-154.6	-296.9	-58.1	2.2×10^{9}	9.3

Table 4.2 $\Delta H, \Delta S, \Delta G$ and K of Bunsen reaction calculated by HSC

$$I_2(l) + SO_2(g) + 2H_2O = H_2SO_4(l) + 2HI(g)$$

T, °C	△H, kJ	△S, J/K	△G, kJ	K	Log(K)
22	106.2	29.1	97.6	5.4×10^{-18}	-17.3
32	105.4	26.7	97.3	2.2×10^{-17}	-16.6
42	104.7	24.4	97.0	8.2×10^{-17}	-16.1
52	104.0	22.2	96.8	2.8×10^{-16}	-15.6

Makitra et al. (2010) reported SO_2 dissolution in toluene. When toluene and water coexist, SO_2 equilibrium among the three phases, gas, water and toluene, can be illustrated in Figure 4.1. When I_2 is brought to the reaction site by the solution of I_2-toluene, I_2 molecules have to diffuse to the interface between the two liquid phases or to the aqueous phase where the reaction takes place. According to the two-film model developed by Lewis and Whitman (1924), the mass transfer direction or the concentration gradient of iodine in this gas-liquid-liquid reaction system is also shown in Figure 4.1.

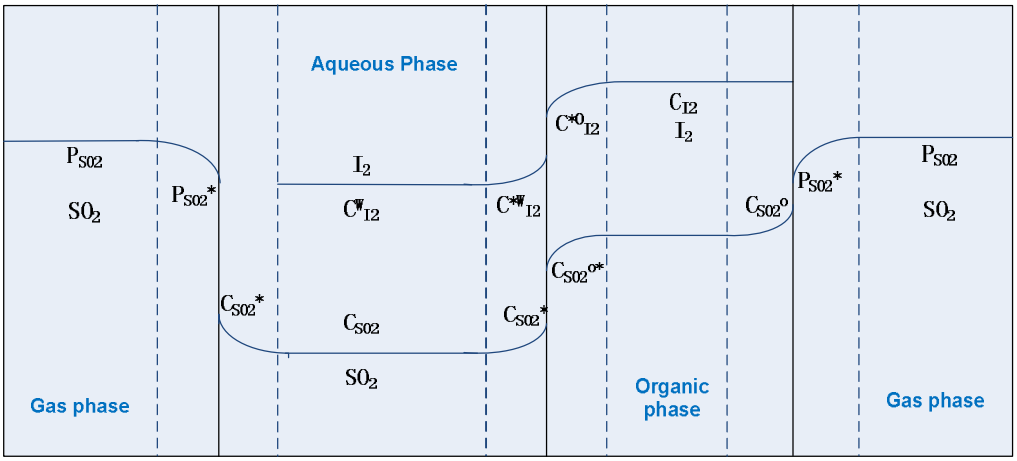

Figure 4.1 Concentration profile of the gas-liquid-liquid Bunsen reaction

In a multiphase reaction system (either gas-liquid-solid or gas-liquid-liquid) in an agitated reactor, the absorption rate of a soluble gas phase reactant is often the rate-limiting step (Poncin et al., 2002). The kinetics of such processes tends to be

complex, for most practical cases, there is no way to determine mass transfer rates and chemical reaction rates separately.

Since only the initial reaction rate is taken into consideration in this study, it is important to analyze the possible rate-limiting steps at time zero. Series of experiments were run to identify how mass transfer and reaction influence the apparent kinetics of the reaction and what the rate-limiting step is.

4.2 Enhancement of rate with Bunsen reaction

Levenspiel (1972) discussed the enhancement of the absorption rate of a gas by adding a reactant to the liquid for the system without gas phase resistance. The enhancement factor was defined as the ratio of the rate with reaction to the rate for mass transfer alone.

As discussed previously, the Bunsen reaction can be described by the two-step mechanism. The first step is the formation of sulfurous acid solution. Because only the initial reaction rate is taken into consideration, it is important to analyze the mass transfer and diffusion features at time zero of the reaction. At time zero, the gas phase contain more than 50 % SO_2 for most of the runs, along with the other half of nitrogen and the ignorable amount of toluene vapor. The total initial pressure of nitrogen and toluene is slightly higher than atmospheric pressure to keep the air out of the reactor

before closing the system. Thus, it is reasonable to assume that the resistance to mass transfer in the gas phase be neglected.

To test the phenomenon of enhancement of the Bunsen reaction to SO_2 dissolving in toluene, the following experiments were conducted. First, with only toluene solvent, the SO_2 dissolving rate was measured at different SO_2 initial partial pressure. Second, the runs were repeated at the same conditions except the liquid phase containing not only toluene but also water and iodine. At 122.7 kPa SO_2 initial partial pressure, the run was also made with toluene and water but not iodine. The details of experiment conditions are giving in the caption of Figure 4.2. The two lines at different conditions almost coincide with each other. Besides, when the SO_2 initial partial pressure is 122.7 kPa, the rate with reaction (toluene+I_2+H_2O), dissolution rate of toluene only and toluene-water are of the same order of magnitude. Hence, there is no significant enhancement of the Bunsen reaction to SO_2 dissolving in toluene, indicating that SO_2 dissolving is the rate-limiting step.

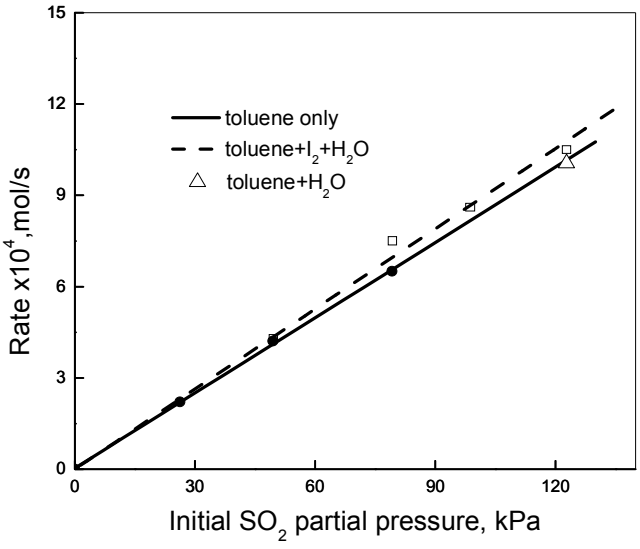

Figure 4.2 Enhancement of rate with Bunsen reaction (22 ^{o}C, 0.7/80 phase ratio, 200 rpm, 80 mL toluene [I_2]: 0.146 mol/L)

4.3 Side reaction considerations

As mentioned in the literature review, Sakurai et al. (2000) reported two side reactions that would occur between the products of the Bunsen section. They are:

$$6HI+H_2SO_4 \rightleftharpoons S+ 3I_2 +4H_2O \quad (2.2)$$

$$8HI+H_2SO_4 \rightleftharpoons H_2S+ 4I_2 +4H_2O \quad (2.3)$$

where sulfur and hydrogen sulfide would be produced. Thus, to test the occurrence of the side reactions at room temperature, the analysis of the substances in both liquid phase and gas phase after typical runs of the reaction rate measurement has been conducted. Unlike the work of Sakurai et al. (2000), where elemental sulfur was easily formed with the increase in acid concentration and the decrease in iodine concentration, no yellow solid

substance, elemental sulfur, was seen in all the runs of my experiments. The gas in the reactor after several typical runs at the lowest and highest temperatures in this study, 22 ^{o}C and 52 ^{o}C was analyzed using gas chromatograph (GC) equipped with the flame photometric detector (FPD). As shown in one of the gas chromatography results in Figure 4.3, no H_2S was detected in the final gas for all the runs measured. The lowest limit of H_2S that the FPD can detect is 0.1 ppm. Therefore, the two side reactions (2.2) and (2.3) that Sakurai et al., (2000) were not detected in this study.

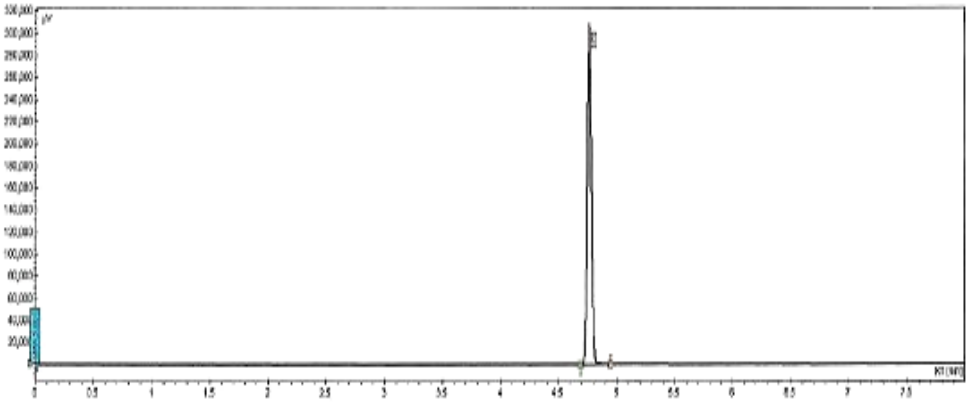

Figure 4.3 GC chromatogram of production of Bunsen reaction

4.4 Uncertainty discussion

4.4.1 Reproducibility of data

It is necessary to test the reliability of the experiment measurements by reproducibility of the data. For this reason, for the typical runs applied to most of the groups, such as the experiment at 22 ^{o}C with 0.7/80 phase ratio, 200 rpm, 122.7 kPa SO_2 initial partial pressure and 0.146 mol/L iodine concentration was repeated. Figure 4.4 shows SO_2 consumption versus time of the three runs under the same condition mentioned above.

The uncertainties of data were analyzed based on Student's t distribution which calculated the confidence interval at 95 %, as eq. (4.3) shows:

$$X = \overline{X} \pm t_{\frac{\alpha}{2}} \frac{s}{\sqrt{n}} \tag{4.3}$$

where $(1-\alpha)\times 100\%$ is the confidence interval needed, $\alpha = 0.5$ as the 95 % confidence interval; $\overline{X}$ represents for the mean value of each measurement, n is the number of measurements and s is the standard deviation. As a result, the concentration of iodine used for the typical runs is 0.146 ± 0.002 mol/L, the SO_2 initial partial pressure is 122.7 ± 2.0 kPa. The initial reaction rate, corresponding to the three runs as Figure 4.4 shows, is 10.5 ± 0.2 mol/s.

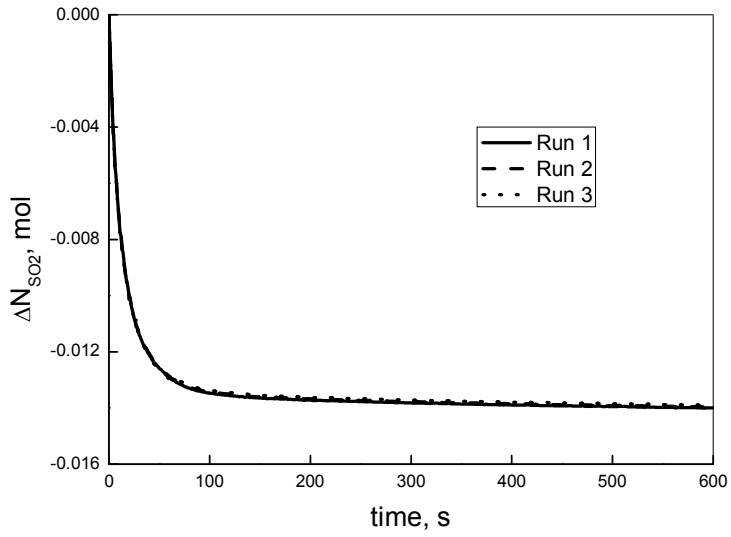

Figure 4.4 Duplicate experiments of Bunsen reaction at 22 ^{o}C (0.7/80 phase ratio, 200 rpm, 122.7 kPa SO_2 initial partial pressure and [I_2]: 0.146 mol/L)

4.4.2 Mass balance

The liquid product including water phase and toluene phase after each run were analyzed by the methods mentioned in Chapter 3. The analysis of various components was repeated three times after each run. Then mass balance for each run was carried out with respect to the ion of iodine. Take four runs as examples, the mass balance for iodine ion is shown in Table 4.3. The iodine mass balance is below 3.29 %, which is also the largest error of all the mass balance for iodine ion. From the mass balance of iodine, all the results of in-out of iodine is above zero, it may be due to the loss of iodine vapor during the reaction. On the other hand, from the last two row of Table 4.3, it can be seen that little amount of iodine was measured in aqueous phase after reaction,

indicating that the iodine diffused from organic phase to aqueous phase during the reaction to supply the reaction.

Table 4.3 Iodine balance for the runs of Bunsen reaction in toluene

$[I_2]$ in toluene mol/L	Iodine in mol	Iodine out mol			in-out	(in-out)/in
	I_2/O	I_2/O	I_2/W	HI/W		
0.146	0.0117	0	0	0.0115	0.0001	0.0128
0.146	0.0234	0	0	0.0226	0.0008	0.0329
0.146	0.0234	0.0067	0.0014	0.0145	0.0007	0.0299
0.195	0.0313	0.0040	0.0020	0.0250	0.0003	0.0102

* I_2/O: iodine in toluene; I_2/W: iodine in water; HI/W: HI in water.

4.5 Effect of volume of liquid

To determine whether the volume of liquid affect the reaction rate measurement, 40 mL I_2-toluene solution with a same iodine concentration and 0.35 mL water were charged into the reactor, compared with the 80 mL I_2-toluene and 0.7 mL water reaction, the phase ratio kept the same. Also, the results, together with the operating conditions, are shown in Table 4.4. The rate is nearly the same no matter how much the volume of both liquids, the reaction rate is independent of the volume of liquids, indicating that Bunsen reaction might not take place inside liquid phases but the interface of the gas and liquid phases.

Table 4.4 Effect of reaction volume on reaction rate
Agitation speed: 100 rpm; SO_2 initial partial pressure: 79.2 kPa;
Reaction temperature: 22 ^oC; $[I_2]$: 0.146 mol/L

I_2+toluene mL	Phase ratio V_W/V_O	rate $\times 10^4$ mol/s
40	0.35/40	5.9
80	0.7/80	6.1

4.6 Effect of phase ratio (V_W/V_O)

As mentioned, one of the objectives of water content study is to reduce the amount of water used in Bunsen reaction, so that the problems caused by large amount of water in the system can be eased. To investigate the effect of volume ratio of water to toluene, experiments were conducted at different phase ratios (V_W/V_O = 0.35/80, 0.7/80, 1.4/80, 2.8/80, 5.6/80) with SO_2 initial partial pressure 79.2 kPa, iodine concentration 0.146 mol/L (Table 4.5a) and SO_2 initial partial pressure 122.7 kPa, iodine concentration 0.2152 mol/L (Table 4.5b) respectively. Here two different SO_2 initial partial pressures were used to monitor the effect of phase ratio, to maintain excess amount of iodine in the system, the iodine concentration used for the two groups of experiment is different consequently. Table 4.5 also shows the mole ratio of water to SO_2 and the corresponding reaction rates. The minimum phase ratio for each group is about the stoichiometric water needed with respect to the SO_2 consumption (N_{H2O}/N_{SO2}=2) in the system. The initial reaction rate is increasing with the phase ratio increased for both groups of experiments,

as Table 4.5 shows. The results can also be obtained from Figure 4.5, which shows the initial reaction rates measured at different phase ratios. It can be seen that at low phase ratio region, the initial rate of reaction increased slowly, at high phase ratio region, this increasing tends to be faster. There is an obvious increasing from phase ratio 1.4/80 to 2.8/80 for both groups of experiments. This phase ratio 2.8/80 can be thus regarded as the desired level of volume ratio of water to toluene, considering reduced water amount is desired for the system.

Figure 4.6 shows the SO_2 consumption with time at 79.2 kPa SO_2 initial partial pressure as an example. In the same reaction time, the consumption amount of SO_2 is nearly the same for each phase ratio. Table 4.6 shows the amount of various components after reaction, such as iodine left in both toluene phase and water phase, the production of iodide and proton after each reaction at 79.2 kPa SO_2 initial partial pressure. The amount of reacted iodine, produced iodide and proton for each phase ratio is nearly constant no matter the phase ratio. However, the mole ratio of iodine unreacted in water phase to that in toluene phase is increasing with the phase ratio increased, indicating that the increased water content may resulted in increased iodine dissolved in water during the reaction.

Table 4.5 Effect of phase ratio on reaction rate
Reaction temperature: 22 °C; Agitation speed: 100 rpm
(a) $[I_2]$: 0.146 mol/L SO_2 init. Pressure: 79.2 kPa;
(b) $[I_2]$: 0.215 mol/L SO_2 init. Pressure: 122.7 kPa

(a)

phase ratio V_W/V_O	N_{H2O}/N_{SO2}	rate $\times 10^4$ mol/s
0.35/80	2	5.7
0.7/80	4	6.1
1.4/80	8	6.5
2.8/80	16	8.1
5.6/80	32	9.6

(b)

phase ratio V_W/V_O	N_{H2O}/N_{SO2}	rate $\times 10^4$ mol/s
0.7/80	2	6.5
1.4/80	4	7.4
2.8/80	8	10.3
5.6/80	16	10.8

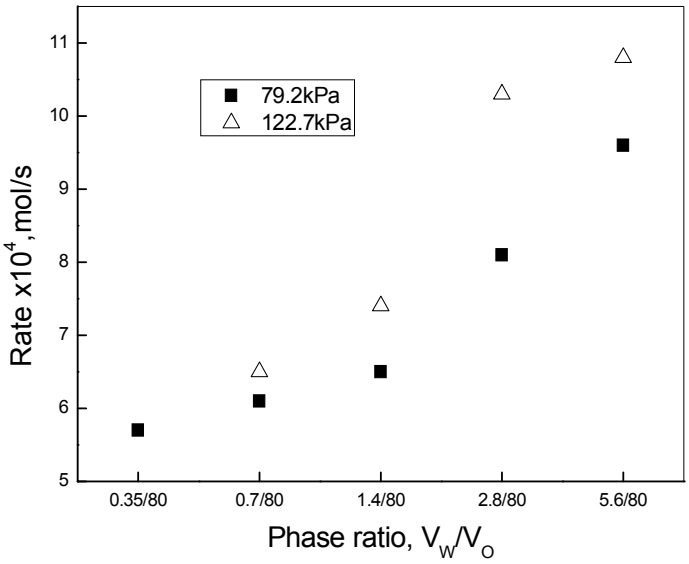

Figure 4.5 Effect of phase ratio (V_W/V_O) on the initial reaction rate (22 ^oC, 100 rpm)

Table 4.6 Amount of various components after reaction with different phase ratio
SO_2 initial partial pressure: 79.2 kPa; [I_2]: 0.146 mol/L

phase ratio V_W/V_O	I_2 left toluene mol	I_2 left water mol	I_2 reacted mol	I^- water mol	H+ water mol
0.35/80	0.0036	0.0006	0.0075	0.0160	0.0297
0.7/80	0.0035	0.0007	0.0074	0.0145	0.0294
1.4/80	0.0035	0.0008	0.0074	0.0148	0.0295
2.8/80	0.0034	0.0008	0.0074	0.0140	0.0295

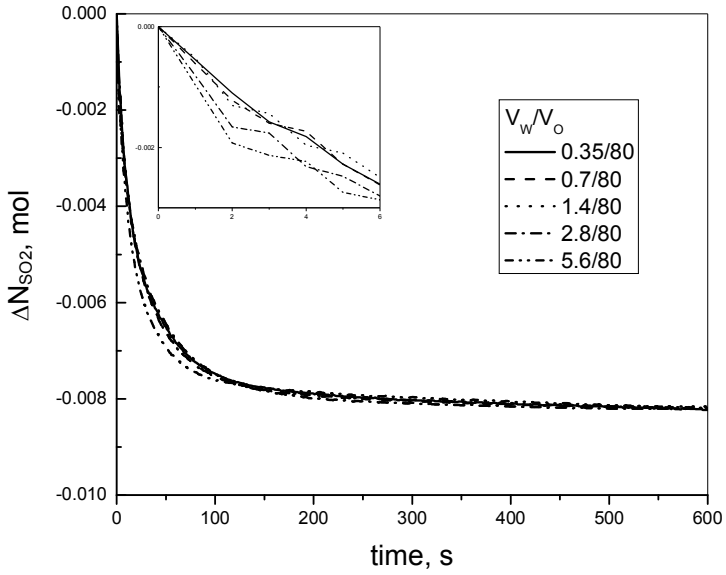

Figure 4.6 SO_2 consumption vs. time at different phase ratio
(79.2 kPa, 22 ^oC, 100 rpm)

It is clearly that, as the phase ratio increased, the initial rate of reaction also increased. Since the interface between aqueous-organic phases has the higher possibility for the reaction to occur, its area would affect the reaction rate undoubtedly. Al-Zuhair et al. (2004) used the microscopic method to determine the size of oil droplets in water for the water-oil agitation system, thus the specific interfacial area of oil-water system could be obtained. Although the accurate quantification of the effective interfacial area was not measured in this study, it is to be expected, as with more amount of water, more interfacial area between aqueous and toluene phase will be generated. The reaction rate then is increasing with the interfacial area increased, which is resulted from the increase of volume ratio of water to toluene. These results are similar to the effects of different

oil ratio on initial reaction rate of oils hydrolysis discussed by Ramachandran et al., (2006), where the interfacial area was determined by the microscopic method proposed by Al-Zuhair et al. (2004).

However, the effect of phase ratio on reaction rate is not limited to the contribution by interfacial area, since water is the reactant in the system, which makes the system more complex.

4.7 Effect of Agitation speed

This section discussed the effects of agitation speed. Firstly, the maximum agitation speed for the system was measured by slowly increasing the agitation speed until the droplet splash appeared. Only 80 mL toluene was used in the determination of maximum agitation speed, and droplet splash appeared at an agitation speed of 425 rpm, indicating that the agitation speed must not exceed 425 rpm. In order to determine the effect of agitation speed on reaction rate, experiments were carried out at 0, 100, 200 and 300 rpm, respectively keeping the other conditions the same. Figure 4.7 shows the photos of the appearance at four different agitation speeds. To make the observation easier, 10 mL water and 70 mL toluene were used for taking photos, with each photo taken after five minutes stirring to allow full development. As Figure 4.7 shows, the water droplets inside the toluene phase are becoming more and smaller with the agitation speed increases. It means the surface area of water droplet is increasing with

the agitation speed increases. This is in agreement with the results reported by Tang et al., (1998) about the interfacial area for gas-liquid-liquid reaction system of water and oil, where the quantitative measurements of interfacial area for different agitation speed was used.

Figure 4.8 shows two sets of data. The solid boxes represent the initial SO_2 dissolving/reaction rate in the mixture of iodine-toluene solution and water at different agitation speeds; the open boxes represent the SO_2 dissolving rate in only toluene. The trend of the rate increase in the former is the same observed with photos: no big difference between 0 and 100 rpm, a significant increase between 100 and 200 rpm, and small increase between 200 and 300 rpm. For an immiscible liquid system, there is always a minimum level of agitation speed above which a uniform dispersion can be produced (Kaul et al., 2007). For our system of toluene and water, 200 rpm can be regarded as the minimum level of agitation to produce a uniform dispersion.

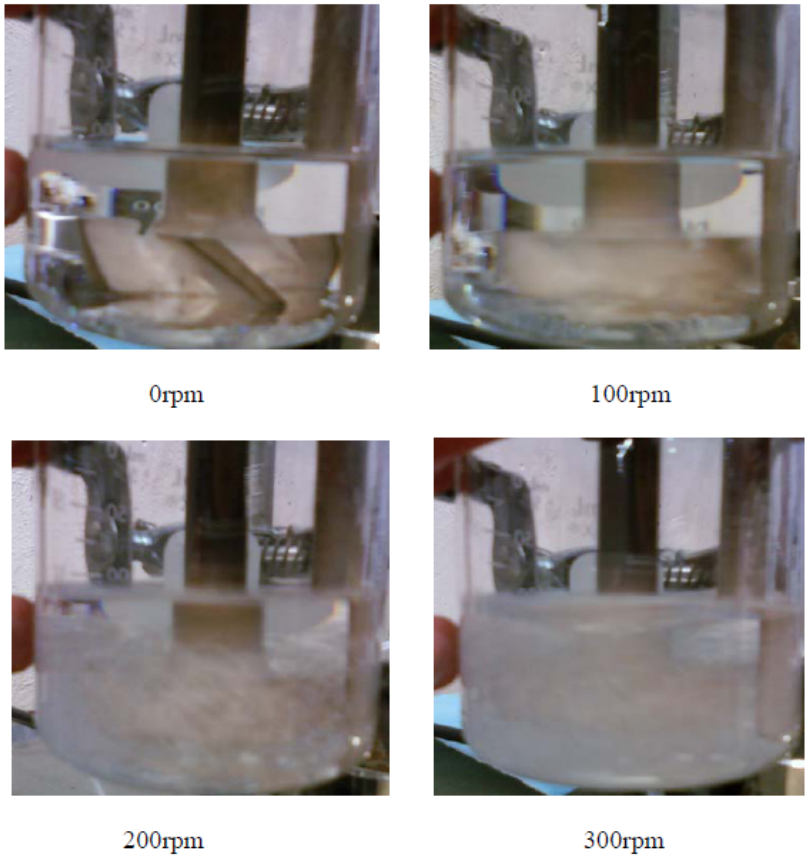

Figure 4.7 Photos of the appearance at four different agitation speeds (V_W/V_O: 10:70)

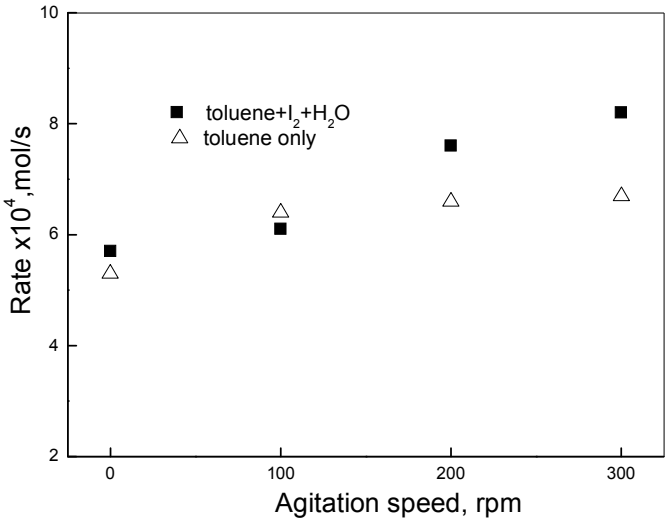

Figure 4.8 Effect of agitation speed on the initial reaction rate (22 ^{o}C, Phase ratio: 0.7/80, $[I_2]$: 0.146 mol/L, SO_2 initial partial pressure: 79.2)

As for the latter, the effect of agitation speed on the SO_2 dissolving rate in only toluene, it is observed that the value of dissolving rate among the four different agitation speeds shows no significant difference, indicating that the dissolution rate is not affected by the agitation speed within the agitation range that this investigation used. This is because the surface area of one phase system is not significant increased by agitation. The comparison between these two sets of data tells that the agitation speed affects the rate when the second phase is added (Dumont et al., 2003).

Figure 4.9 shows the plots of SO_2 consumption versus time for 0, 100, 200 and 300 rpm respectively. In the same reaction time, the consumption amount of SO_2 is

increasing with the agitation speed increased. The observation shows a strong dependence of the conversion of reactant on agitation speed. This can be confirmed by the consumption of iodine in each phase ratio, as shown in Table 4.7. The amount of reacted iodine, produced iodide and proton are increasing with the agitation increased for 40 minutes of operation. This behavior is similar to what was shown by the agitation effects study for methyl ethyl ketazine production reaction (Kaul et al., 2007), also a gas-liquid-liquid system, where the percentage conversion is found to increase with increasing stirring speed for 6 hours of operation.

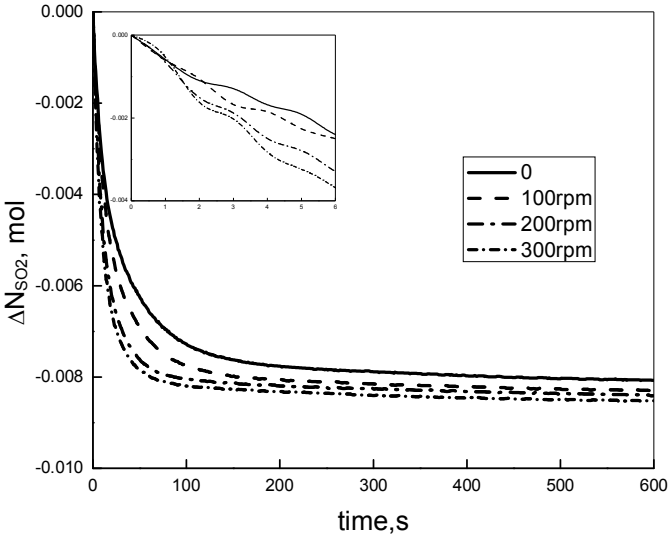

Figure 4.9 SO_2 consumption vs. time for different agitation speed (22 ^oC, Phase ratio: 0.7/80, $[I_2]$: 0.146 mol/L, SO_2 initial partial pressure: 79.2)

Table 4.7 Amount of various components after reaction for different agitation speed reaction time: 40mins

Agitation speed rpm	I_2 left toluene mol	I_2 left water mol	I_2 reacted mol	I^- water mol	H^+ water mol
0	0.0045	0.0012	0.0059	0.0126	0.0231
100	0.0039	0.0009	0.0069	0.0140	0.0274
200	0.0034	0.0009	0.0074	0.0148	0.0294
300	0.0024	0.0008	0.0084	0.0160	0.0335

As shown in the results for the agitation effect, the agitation affects the reaction rate, indicating that the chemical reaction is not the rate determining factor definitely, since for the system controlled only by chemical reaction, the degree of agitation has no effect on reaction rate (Carpenter, 1986).

Above all, the initial reaction rate is found to increase with increase in phase ratio (V_W/V_O) and agitation speed respectively. Although, the specific interfacial area was not investigated in this study, the effect of volume ratio of the two immiscible liquid and agitation speed on interfacial area for a gas-liquid-liquid system is supported by abundant literature. Thus, the initial reaction rate is increasing with the interfacial area increased. Although agitation can increase the speed of surface renewal, only initial reaction rate is taken into account for this study, the role of surface renewal could be negligible. (Kaur et al., 2007).

Besides, the effect of temperature on interfacial area is neglected. Usually the viscosity reduction of liquid due to the increase in temperature would change the interfacial area (Calderbank, 1958). But the viscosity data of toluene between 22 and 52 ^{o}C won't change significantly. The viscosity of toluene is 0.580 cP for 20 ^{o}C and 0.412 cP for 50 ^{o}C (Lide, 2007), also Al-Zuhair et al., (2004) showed that the change of interfacial area for the water-oil system with temperature is small with a low agitation speed (<500 rpm). Thus, temperature change will not change the interfacial area in the temperature range.

4.8 Establishment of effective interfacial area and kinetic equation

As discussed above, the reaction rate is increased by 58 % when the phase ratio increases from 0.7/80 to 5.6/80 and by 37 % when the agitation speed increases from 0 rpm to 300 rpm. To quantify the effect of momentum, the increased of rate by agitation and phase ratio is considered only to the increase of interfacial area. However, the accurate interfacial area for a gas-liquid-liquid reaction is difficult to measure. To establish the kinetic equation (eq. 4.4) of the reaction and make the reaction rate in a standard unit magnitude, we use an effective interfacial area.

$$-r_{SO_2} = ka_{eff}\left[I_2\right]^m P_{SO_2}^n \tag{4.4}$$

The effective area is defined to be a function of the volume of liquid, the volume ratio of water to toluene, the agitation speed and the temperature. The temperature effect has been neglected. The earlier discussion has indicated that, the reaction rate is independent of liquid volume within the range of interest. Thus, agitation speed and phase ratio are the only two factors to be taken into consideration. To quantify the effective interfacial area, the cross sectional area of the glass liner in the reactor, 0.00255 m^2, is used as the base of the interfacial area when the system is at the zero agitation speed, 80 mL liquid volume and the V_W/V_O of 0.7:80. If at any other condition, the initial reaction rate changes due to the agitation speed or the change in liquid volume or the volume ratio of water to toluene, the change of the effective interfacial area can be determined according to the change of the initial reaction rate. Based on this analysis, the effective interfacial

areas at various agitation speeds and water to toluene volumetric ratio are listed in Table 4.8.

Table 4.8 Effective interfacial area at various conditions

Agitation speed rpm	Phase ratio V_W/V_O	Effective interfacial area ($a_{eff}\times10^3$), m^2
0	0.7/80	2.55
100	0.7/80	2.64
200	0.7/80	3.25
300	0.7/80	3.49
100	0.35/80	2.30
100	1.4/80	2.73
100	2.8/80	3.47
100	5.6/80	4.03

4.9 Effect of concentration of iodine

To study the effect of iodine concentration on initial reaction rate, experiments were conducted at the iodine concentrations of 0.235, 0.195, 0.146, 0.118, 0.078 and 0.045 mol/L at 22 ^{o}C and 52 ^{o}C, respectively. The specific conditions and their corresponding initial reaction rates are shown in Table 4.9. SO_2 is excessive for the runs of 0.195, 0.146, 0.118, 0.078 and 0.045 mol/L iodine concentrations. From the results in Table 4.9, it is clear that the greater the iodine concentration, the greater the initial reaction rate at both temperatures. Afterwards, the relationship between reaction rate and iodine concentration at both 22 ^{o}C and 52 ^{o}C was plotted, respectively, in Figure 4.10. The observation shows a strong dependence of reaction rate on iodine concentration. It can be seen that at low iodine concentrations, the initial rate of reaction increased linearly. At high iodine concentrations, this linear relationship tends to be flattened. This appears that when the iodine concentration is high, the interface between aqueous phase and toluene phase could be saturated with the iodine molecules (Ramachandran et al., 2006). Thus, any further increase in iodine concentration in the bulk could not enhance the initial reaction rate any more. In general, an increase in the bulk iodine concentration would increase the initial reaction rate, but there would be a critical iodine concentration at which the interfacial area would be saturated with the iodine. For this study, 0.146 mol/L could be considered as the critical iodine concentration. These results are in agreement with those revealed by Al-Zuhair et al.,

(2004) about enzyme concentration on reaction rate of hydrolysis of oils. In the mechanism aspect, with a greater iodine concentration, more iodine is available in reaction mixture, and thus more iodine is in the aqueous layer to react.

Figure 4.11 shows the plots of SO_2 consumption versus time for 0.235, 0.195, 0.146, 0.118, 0.078 and 0.045 mol/L respectively at 22 ^oC, the consumption of SO_2 in a same time only has little difference for different iodine concentration.

Table 4.9 Effect of iodine concentration on reaction rate
Phase ratio: 0.7/80; Agitation speed: 200 rpm N_{H2O}/N_{SO2}: 2
Reaction temperature: (a) 22 ^{o}C; (b) 52 ^{o}C

(a)

$[I_2]$ in toluene mol/L	N_{SO2}/N_{I2}	SO_2 init. pres kPa	rate $\times 10^4$ mol/s
0.235	0.8	122.7	11.3
0.195	1	122.7	11.0
0.146	1.3	122.7	10.5
0.118	1.6	122.7	9.8
0.078	2.5	122.7	8.8
0.045	4.3	122.7	8.1

(b)

$[I_2]$ in toluene mol/L	N_{SO2}/N_{I2}	SO_2 init. pres kPa	rate $\times 10^4$ mol/s
0.195	1	122.7	14.0
0.146	1.3	122.7	13.4
0.118	1.6	122.7	12.3
0.078	2.5	122.7	10.4
0.045	4.3	122.7	9.5

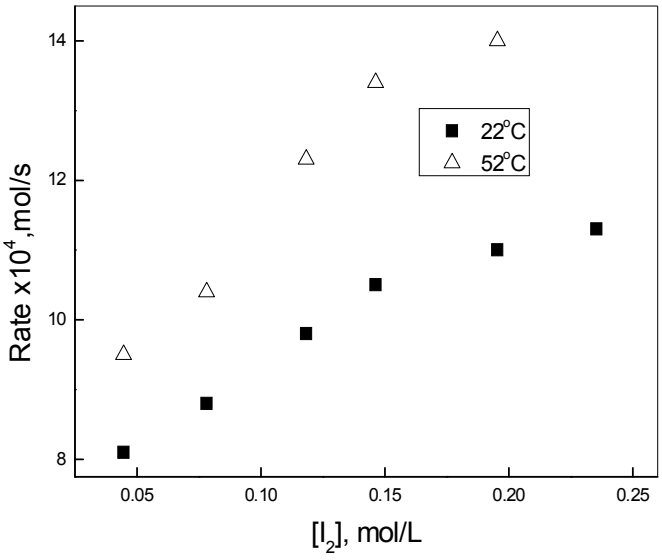

Figure 4.10 Effect of iodine concentration on the initial reaction rate (Phase ratio: 0.7/80; 200rpm, SO_2 initial partial pressure: 122.7 kPa)

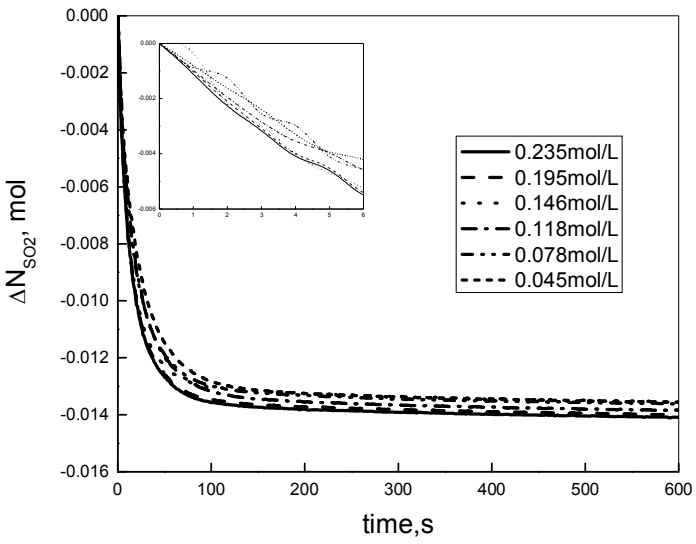

Figure 4.11 SO_2 consumption vs. time for different iodine concentration (22 ^oC, Phase ratio: 0.7/80; 200rpm, SO_2 initial partial pressure: 122.7 kPa)

Figure 4.12 adds the SO_2 dissolution rate in toluene only and in toluene and water at 200 rpm agitation speed, 22 ^oC and SO_2 initial partial pressure of 122.7 kPa to the plot of the reaction rate at different iodine concentration. Above 0.15 mol/L of iodine in toluene, the reaction rate is bigger than the dissolution rate of SO_2 in toluene and in toluene and water mixture, while below this concentration, the reaction rate is smaller than the dissolution rate. The improved reaction rate can be explained by the enhancement effect; however, not any reliable explanation was developed.

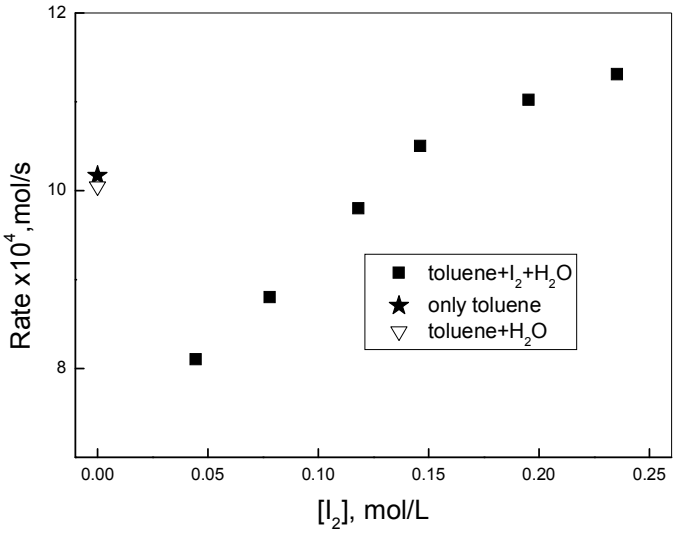

Figure 4.12 Effect of coexistence of T-W-I_2 on SO_2 dissolution rate (22 ^oC, Phase ratio: 0.7/80; 200rpm, SO_2 initial partial pressure: 122.7 kPa)

4.10 Effect of initial partial pressure of SO_2

As one of the reactants, the initial partial pressure of SO_2 must be a factor which affects the initial reaction rate. To investigate the influence of the SO_2 initial partial pressure on the initial reaction rate, experiments were conducted at the SO_2 initial partial pressure of 122.7, 98.7, 79.2 and 49.6 kPa at both 22 ^oC and 52 ^oC. The other conditions are water to toluene volumetric ratio 0.7:80, 80mL volume of I_2-toluene, 0.146 mol/L iodine concentration and 200 rpm agitation speed. The iodine is excessive for the runs of 98.7, 79.2 and 49.6 kPa. The initial reaction rates versus SO_2 initial partial pressure are shown in Table 4.10. The plots of SO_2 consumption vs. time for 122.7, 98.7, 79.2 and 49.6 kPa at 22 ^oC respectively, are shown in Figure 4.13.

From the results in Table 4.10, it is clear that the greater the SO_2 initial partial pressure, the greater the initial reaction rate. Afterwards, the relationship between reaction rate and SO_2 initial partial pressure at both temperatures was plotted in Figure 4.14. It can be seen the initial rate of reaction increased linearly.

Table 4.10 Effect of SO_2 initial partial pressure on reaction rate
Phase ratio: 0.7/80; $[I_2]$: 0.146 mol/L Agitation speed: 200 rpm
Reaction temperature: (a) 22 ^oC; (b) 52 ^oC

(a)

SO_2 init. pres kPa	N_{SO2}/N_{I2}	rate $\times 10^4$ mol/s
122.7	1.3	10.5
98.7	1	8.5
79.2	0.8	7.6
49.6	0.5	4.3

(b)

SO_2 init. pres kPa	N_{SO2}/N_{I2}	rate $\times 10^4$ mol/s
122.7	1.3	13.4
98.7	1	10.7
79.2	0.8	8.9
49.6	0.5	4.9

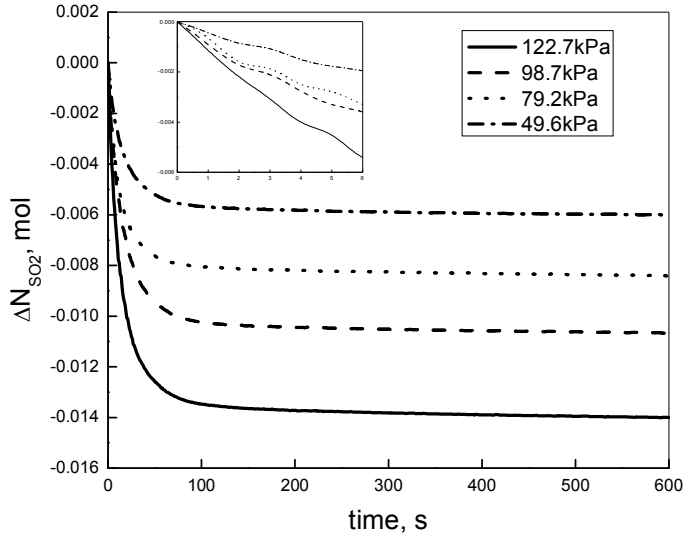

Figure 4.13 SO_2 consumption vs. time for different SO_2 initial partial pressure (22 ^oC, Phase ratio: 0.7/80; 200rpm, $[I_2]$: 0.146 mol/L)

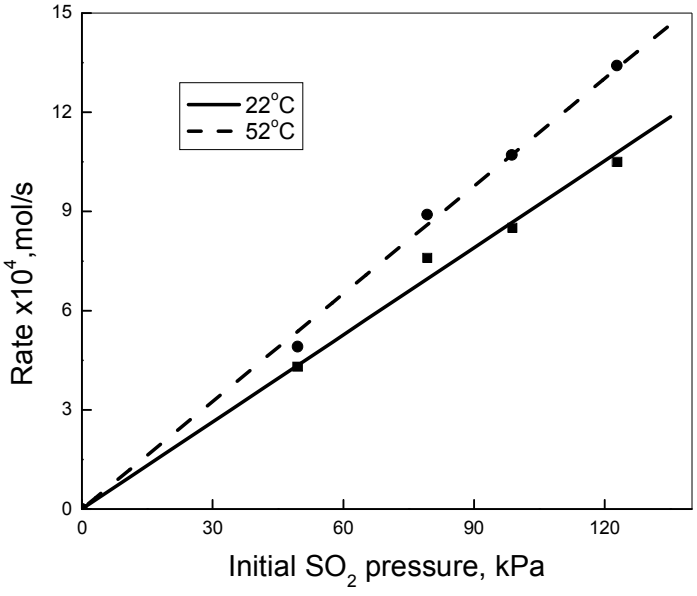

Figure 4.14 Plots of initial reaction rate vs. initial SO_2 pressure for different T (Phase ratio: 0.7/80; 200rpm, $[I_2]$: 0.146 mol/L)

4.11 Specific reaction rate for Bunsen reaction in the presence of toluene

The values of kinetic parameters such as the specific reaction rate, k, the orders with respect to iodine and sulfur dioxide, m and n, in the rate equation,

$$-r_{SO_2} = ka_{eff}\left[I_2\right]^m P_{SO_2}^n \tag{4.4}$$

can be determined from the experimental data. Firstly, at a given iodine concentration 0.146 mol/L, the initial rates at various SO_2 initial partial pressures from 49.6 kPa to 122.7 kPa at two temperatures of 22 ^oC and 52 ^oC are listed in Table 4.10. The order of the reaction with respect to the partial pressure of SO_2 was obtained by correlating the initial reaction rates with the initial partial pressure. As an example, the results at 0.146 mol/L concentration of iodine at 22 ^oC and 52 ^oC are shown in Figure 4.14. This figure clearly demonstrates a first order behavior with respect to SO_2 at both temperatures of 22 ^oC and 52 ^oC, *i.e.*,

$$-r_{SO_2} = k'P_{SO_2} \tag{4.5}$$

The slopes from the linear regression correspond to the value of k' at a given iodine concentration. k' values at the two temperatures are shown in Table 4.11.

Table 4.11 Values of k' in Equation (4.5)

T, ^oC	$k' \times 10^6$, mol s^{-1} kPa^{-1}	R^2
22	8.8±0.2	0.9946
52	10.8±0.2	0.9974

Then attempts were made to correlate the reaction rate at a given pressure of SO_2 pressure with the iodine concentration in order to determine the values of the reaction order, *m*, with respect to iodine concentration. The linear portion of Figure 4.10 was replotted in Figure 4.15. Because the reaction rate is linear proportional to the iodine concentration in the low iodine concentration region, this figure clearly illustrates a first order behavior with respect to iodine concentration in the low concentration region at both temperatures. But the lines do not pass through the origin point. Both linear regressions can be described by

$$-r_{SO_2} = k''([I_2]+C) \tag{4.6}$$

where the slopes of the linear regression curve correspond to the value of k'' at a given SO_2 initial partial pressure and the two temperatures. The k'' values are shown in Table 4.12. The values of the slopes are 0.002374 and 0.003869 L s^{-1}, respectively for 22 and 52 ^{o}C, indicating the first order with respect to the iodine concentration at both temperatures. The intercepts of $k''C$ generated in Eq. (4.6) may be contributed by both dissolving and reaction. As discussed of the blank experiment, it is clear the initial rate is not zero when there is no iodine in the system. Thus, it is reasonable to have the constant C in Eq. (4.6) by correlating the initial reaction rates with the iodine concentration.

Table 4.12 Values of k'' and C in Equation (4.6)

T, ^{o}C	$k'' \times 10^3$, L s^{-1}	C, mol/L	R^2
22	2.4±0.1	0.30±0.01	0.9984
52	3.9±0.1	0.20±0.03	0.9906

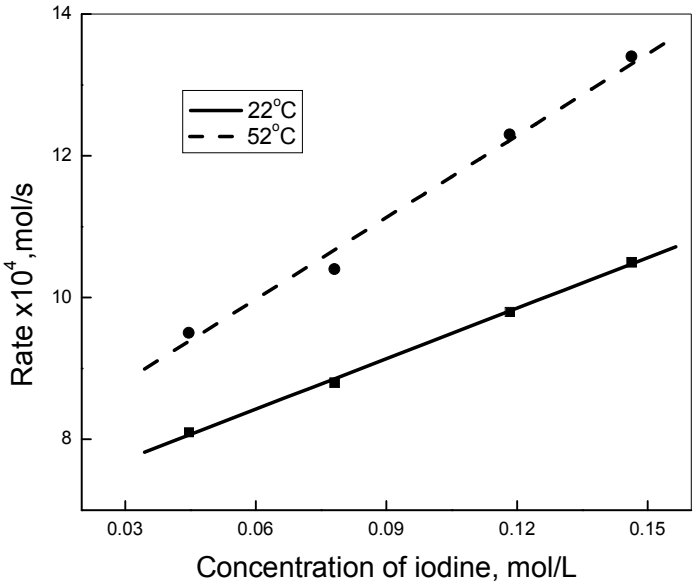

Figure 4.15 Plots of initial reaction rate vs. iodine concentration for different T (Phase ratio: 0.7/80; 200 rpm, SO_2 initial partial pressure: 122.7 kPa)

As a result from the above discussion, the reaction rate equation, Eq. (4.4) can be modified to the following equation:

$$-r_{SO_2} = ka_{eff} P_{SO_2} ([I_2] + C) \tag{4.7}$$

Based on Eq. (4.7), Eq. (4.5) and (4.6) can be modified to Eq. (4.8) or Eq. (4.9) respectively:

$$-r_{SO_2} = \frac{k'}{[I_2] + C} P_{SO_2} ([I_2] + C) \tag{4.8}$$

$$-r_{SO_2} = \frac{k''}{P_{SO_2}} ([I_2] + C) P_{SO_2} \tag{4.9}$$

Compared with Eq. (4.7), ka_{eff} corresponds to $\frac{k'}{[I_2] + C}$ in Eq. (4.8) and $\frac{k''}{P_{SO_2}}$ in Eq. (4.9). Take the results at 22 ^{o}C from Table 4.11 and 4.12 as an example, the calculations are as followings:

When $[I_2]$ =0.146 mol/L,

$$ka_{eff} = \frac{k'}{[I_2] + C} = \frac{8.8 \times 10^{-6}}{0.146 + 0.30} = 1.97 \times 10^{-5} \, \mathrm{L \cdot kPa^{-1} \cdot s^{-1}}$$

When P_{SO_2} =122.7 kPa,

$$ka_{eff} = \frac{k''}{P_{SO_2}} = \frac{2.4 \times 10^{-3}}{122.7} = 1.93 \times 10^{-5} \, \mathrm{L \cdot kPa^{-1} \cdot s^{-1}}$$

The ka_{eff} calculated from the two equations with different sets of experiment changing either SO_2 initial partial pressure or iodine concentration is nearly the same. As discussed earlier, the effective interfacial area under such conditions is 0.00325 m^2, and then the specific reaction rate k can be obtained. Theoretically, the constant C is not a

function of temperature, so we average the two value of C, 0.25, as part of the final rate equation:

$$-r_{SO_2} = ka_{eff} P_{SO_2} ([I_2] + 0.25) \tag{4.10}$$

The earlier, discussion shows that water is not only a reactant in the Bunsen reaction, but also provides effective interface to the reaction. Thus, it is difficult to work out a simple order of reaction with respect to water.

4.12 Effect of temperature on initial reaction rate

To study the effect of temperature on initial reaction rate, two more runs were conducted at 32 and 42 ℃ respectively with certain iodine concentration and SO_2 initial partial pressure. The specific conditions and their corresponding initial reaction rates and specific reaction rate calculated from Eq. (4.10) are given in Table 4.13. From Table 4.13, it is clear that as temperature increases, the specific initial reaction rate increases. The temperature dependence of the reaction can be determined using Arrhenius equation. The relationship between k and temperature T may be described by

$$k = A_0 \exp(-\frac{E_a}{RT}) \tag{4.11}$$

where, the activation energy of the reaction can be obtained by correlating the specific reaction rate and the reciprocal of absolute temperature, as shown in Figure 4.16. The activation energy calculated is (6.02 ± 0.14) kJ/mol according to Figure 4.16. The

Preexponential factor $\ln A_0$ is -9.46 ± 0.06. The reaction rate shows light dependence on temperature, furthermore, the activation energy is much lower than a normal chemical reaction. It suggests that the reaction process should be controlled by SO_2 dissolving.

Table 4.13 Effect of temperature on initial reaction rate
Phase ratio (V_W/V_O):0.7/80; Agitation speed: 200 rpm

Temperature ^oC	SO_2 init. pres kPa	$[I_2]$ in toluene mol/L	rate $\times 10^4$ mol/s	$k \times 10^6$ m $s^{-1}kPa^{-1}$
22	122.7	0.118	9.8	6.7
32	122.7	0.118	10.7	7.3
42	122.7	0.118	11.5	7.8
52	122.7	0.118	12.3	8.4

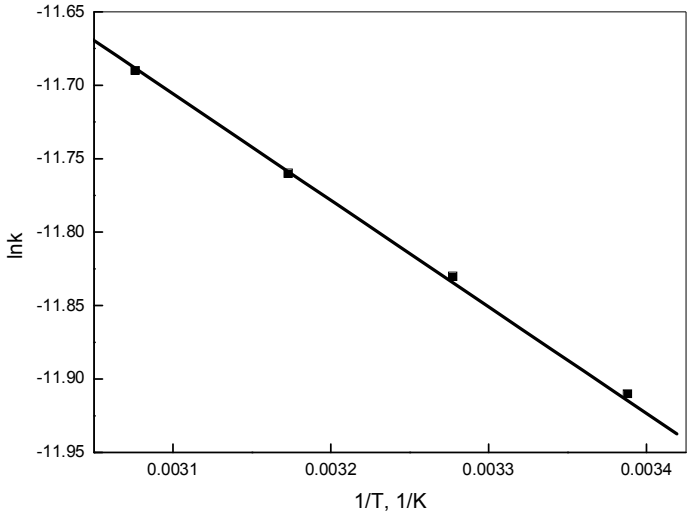

Figure 4.16 Arrhenius plot for Bunsen reaction in the presence of toluene
(Phase ratio: 0.7/80; 200rpm, $[I_2]$: 0.146 mol/L, SO_2 initial partial pressure: 122.7 kPa)

CHAPTER 5

CONCLUSIONS AND FUTURE WORK

In the research of H_2S splitting cycle for hydrogen production, the kinetics of Bunsen reaction, especially in the presence of toluene was explored. The followings were concluded:

1. The reaction rate was found to be the first order with respect to SO_2 and I_2 respectively under certain conditions. A rate equation was established in which SO_2 and I_2 are involved. The results of temperature effect show that the reaction followed the Arrhenius equation with an activation energy of 6.02 kJ/mol.

2. Both of the agitation and water/toluene volume ratio affect the reaction rate. The 200 rpm of agitation speed was regarded as the minimum level desired for agitation. Water/toluene volume ratio 2.8:80 was regarded as the desired level of water content, considering reduced water amount is desired for the system.

3. The iodine diffused from organic phase to aqueous phase during the reaction since little amount of iodine was measured in aqueous phase after reaction. Bunsen reaction has no significant enhancement to the dissolution of SO_2. The dissolution of SO_2 and chemical reaction are of the same order of magnitude. Moreover, the agitation plays a significant role in increasing the reaction rate, indicating that the chemical

reaction must not be the rate-limiting step. The magnitude of the small activation energy also suggests that the reaction is controlled by SO_2 dissolution.

4. Therefore, the Bunsen reaction rate in the gas-liquid-liquid system as discussed in this thesis can be improved by enhancing the SO_2 dissolving rate.

It is recommended that other reactors that are able to largely enhance the mass transfer among phases be used in the future study. Other solvents such as xylenes that have higher iodine solubility should be taken into consideration.

REFERENCE

Al-Zuhair S., K.B. Ramachandran and M. Hasan (2004). Investigation of the specific interfacial area of a palm oil–water system. Chem. Technol. Biotechnol., 79, 706-710.

Beenackers A.A.C.M. and W.P.M. van Swaaij (1993). Mass transfer in gas–liquid slurry reactors: a critical review. Chem. Eng. Sci.,48(18), 3109-3139.

Brown L.C., G.E. Besenbruch and K.R. Schultz et al. (2002). High Efficiency Generation of Hydrogen Fuels Using Thermochemical Cycles and Nuclear Power, GA-A24326, General Atomics.

Brown L.C., J.F. Funk and S.K. Showalter (2000). Initial Screening of Thermochemical Water-Splitting Cycles for High Efficiency Generation of Hydrogen Fuels Using Nuclear Power, GAA23373, General Atomics.

Calabrese V.T. and A. Khan (2000). Polyiodine and Polyiodide Species in an Aqueous Solution of Iodine+KI: Theoretical and Experimental Studies. J. Phys. Chem. A., 104:1287-1292.

Calderbank P. H. (1958). Physical rate processes in industrial fermentation, Part I: The interfacial area in gas–liquid contacting with mechanical agitation. Trans. Inst. Chem. Eng., 36, 443-463.

Carpenter K.J. (1986). Fluid Processing in Agitated Vessel. Chem. Engg. Res. Des., 64(1), 3-10.

Danckwerts P.V. (1970). Gas-Liquid Reactions, McGraw-Hill, New York.

De Beni G., G. Pierini and B. Spelta (1980). The Reaction of Sulfur Dioxide with Water and a Halogen. The Case of Iodine: Reaction in Presence of Organic Solvents. Int. J. Hydrogen Energy, 5, 141-149.

Dumont E. and H. Delmas (2003). Mass transfer enhancement of gas absorption in oil-in-water systems: a review. Chemical Engineering and Processing, 42, 419-438.

Gamson B.W. and R.H. Elkins (1953). Sulfur from Hydrogen Sulfide. Chem. Eng. Progr.,

49(4), 203-215.

Giaconia A., G. Caputo and A. Ceroli et al. (2007). Experimental Study of Two Phase Separation in the Bunsen Section of the Sulfur-Iodine Thermochemical Cycle. Int. J. Hydrogen Energy, 32, 531-536.

Giaconia A., G. Caputo and S. Sau et al. (2009). Survey of Bunsen reaction routes to improve the sulfur–iodine thermochemical water-splitting cycle. Int. J. Hydrogen Energy, 34, 4041-4048.

Goldstein S., J.M. Borgard and X. Vitart (2005). Upper bond and best estimate of the efficiency of the iodine sulfur cycle. Int. J. Hydrogen Energy, 30, 619-626.

Guo H.F., P. Zhang and Y. Bai et al. (2010). Continuous purification of H_2SO_4 and HI phases by packed column in IS process. Int. J. Hydrogen Energy, 35, 2836-2839.

Hildebrand J.H., J.H. Benesi and L.M. Mower (1950). Solubility of iodine in Ethyl Alcohol, Ethyl Ether, Mestilylene, p-xylene, 2,2-dimethylbutane, Cyclohexane, and Perfluoro-n-heptane, J. Am. Chem. Soc., 72(12), 1017-1020.

Hu L. and A.A. Adeyiga (2002). Kinetics Model of Gas-Liquid-Liquid Decomposition Extraction. Ind. Eng. Chem. Res., 41, 5584-5593.

Jolly, William L. (1991), Modern Inorganic Chemistry (2nd ed.), New York: McGraw-Hill.

Kaur R., R. Machiraju and K.D.P. Nigam (2007). Agitation effects in a gas- liquid- liquid reactor system: methyl ethyl ketazine production. Int. J. Chem. React. Eng., 5, A27.

Le Person A. (2008). Unpublished report.

Levenspiel O. (2007). Chemical Reaction Engineering. 2nd Edition.

Lewis W.K. and W.G. Whitman (1924). Principles of gas absorption, Ind. Eng. Chem., 16, 1215-1220.

Lide D.R. (2007). CRC Handbook of Chemistry and Physics. 87th Edition.

Lu S., L. Wang, Y. Wang and Z. Mi (2011). Kinetic Model of Gas-Liquid-Liquid Reactive Extraction for Production of Hydrogen Peroxide. Chem. Eng. Technol., 34, 5, 823-830.

Makitraa R.G., S.D. Kal'muka, D.V. Bryka and I.P. Polyuzhinb (2010). Factor Controlling Sulfur Dioxide solubilities in Organic solvents. Russian Journal of Inorganic Chemistry, 55(8), 1322-1329.

Mizuta S. and T. Kumagai (1990). Continuous flow system demonstration and evaluation of thermalefficiency for the magnesium-sulphur-iodine thermochemical water-splitting cycle. Ind. Eng.Chem. Res., 29, 565-571.

Nomura M., S. Fujiwara and K. Ikenoya et al. (2004a). Application of an Electrochemical Membrane Reactor to the Thermochemical Water Splitting IS Process. J. Memb. Sci., 240, 221-226.

Nomura M. and S. Nakao (2004b). Development of an Electrochemical Cell for Efficient Hydrogen Production through the IS Process. AIChE J., 50, 1991-1998.

Norman J.H., G.E. Besenbruch and D.R. O'Keefe (1981). Thermochemical water-splitting for hydrogen production. Gas Research Institute, GRI-80/0105.

O'Keefe D.R., C. Allen and G. Besenbruch et al. (1982). Preliminary Results from Bench-Scale Testing of a Surlfur-Iodine Thermochemical Water-Splitting Cycle. Int. J. Hydrogen Energy, 7, 381-392.

Poncin S, C. Nguyen, N. Midoux and J. Breysse (2002). Hydrodynamics and volumetric gas–liquid mass transfer coefficient of a stirred vessel equipped with a gas-inducing impeller. Chem. Engg. Sci., 57(16), 3299-3306.

Powell C.F. and I.E. Campbell (1947). The Solubility of Iodine in Concentrated Hydriodic Acid Solutions. J. Am. Chem. Soc., 69 (5), 1227-1228.

Ramachandran K.B., S. Al-Zuhair, C.S. Fong and C.W. Gak (2006). Kinetic study on hydrolysis of oils by lipase with ultrasonic emulsification. J. Biochem. Eng., 32, 19-24.

Roth M. and K.F. Knoche (1989). Thermochemical Water Splitting through Direct HI-Decomposition from $H_2O/HI/I_2$ Solutions. Int. J. Hydrogen Energy, 14, 545-549.

Sakurai M., H. Nakajima, A. Rusli, K. Onuki, S. Shimizu (2000). Experimental study on side-reaction occurrence condition in the sulfur–iodine thermochemical hydrogen

production process. Int. J. Hydrogen Energy, 25, 613-619.

Sau S., A. Giaconia and G. Caputo et al. (2008). Decrease the Rate of Recycling Agents in the Sulfur-Iodine Cycle by Solid Phase Separation. Int. J. Hydrogen Energy, 33, 6439-6444.

Tang W., Y. Zhu and C. Song (1998). Determination of interfacial areas in high-speed stirring apparatus. J. Tsinghua University (Sci & Tech), 7, 58-61.

Vitart X., A. Le Duigou and P. Carles (2006). Hydrogen production using the sulfur-iodine cycle coupled to a VHTR: an overview. Energy Convers. Manage, 47, 2740-2747.

Wang H., I.G. Dalla Lana and K.T. Chuang (2002a). Kinetics and mechanism of oxidation of hydrogen sulfide by concentrated sulfuric acid. Ind. Eng. Chem. Res., 41, 6656-6662.

Wang H., I.G. Dalla Lana and K.T. Chuang (2002b). Kinetics of Reaction between Hydrogen Sulfide and Sulfur Dioxide in Sulfuric Acid Solutions. Ind. Eng. Chem. Res., 41, 4707-4713.

Wang H, I.G. Dalla Lana and K.T. Chuang (2003). Thermodynamics and Stoichiometry of Reactions between Hydrogen Sulfide and Concentrated Sulfuric Acid. Can. J. Chem. Eng., 81, 80-85

Wang, H. (2007). Hydrogen production from a chemical cycle of H_2S splitting. Int. J. Hydrogen Energy, 32, 3907-3914.

Wang H. (2008). Personal communication.

Yang L. (2010). The Bunsen reaction in the presence of organic solvent in H_2S splitting cycle. Thesis of Master of University of Saskatchewan.

Zhang P., S.Z. Chen, L.J. Wang and J.M. Xu (2010). Overview of nuclear hydrogen production research through iodine sulfur process at INET. Int. J. Hydrogen Energy, 35, 2883-2887.

Zhang Q., I.G. Dalla Lana, K. T. Chuang and H. Wang (2000). Reactions between Hydrogen Sulfide and Sulfuric Acid: a Novel Process for Sulfur Removal and Recovery. Ind. Eng. Chem. Res., 39, 2505-2509.

APPENDIX A
Measurements of I_2 and I^- by UV-Vis

The concentrations of iodine in toluene and iodide in water were measured by UV-Vis, using Beer Lambert law, the concentration of iodine and iodide can be calculated according to the absorbance:

$$A = -\lg\frac{I}{I_0} = \varepsilon \cdot 1 \cdot c$$

The peak used is the one at 496 nm for iodine in toluene (Figure B.1) and that 226 nm (Figure B.2) for iodide in water. The absorbance is increasing with the concentration. With known concentrations and their responding absorbance for both iodine and iodide, UV-Vis calibration curves can be plotted in Figure B.3 (Iodine) and Figure B.4 (Iodide), respectively. The slopes of the linear regressions are the molar extinction coefficients, respectively, which is 1.025×10^3 L $mol^{-1}cm^{-1}$ for iodine and 1.33×10^4 L $mol^{-1}cm^{-1}$ for iodide.

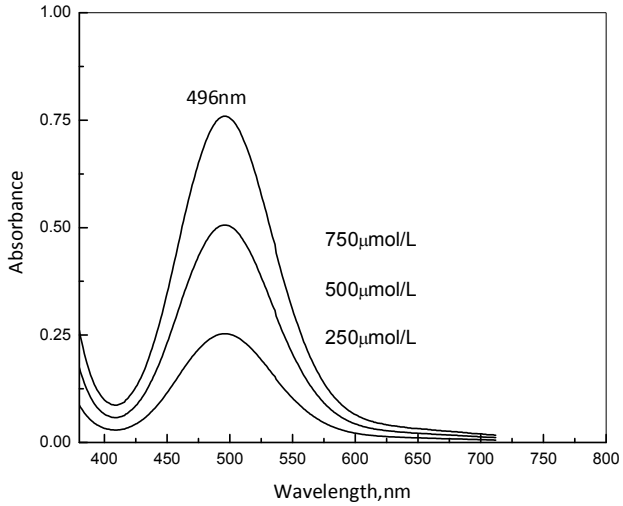

Figure A.1 Absorption spectrum of iodine in toluene

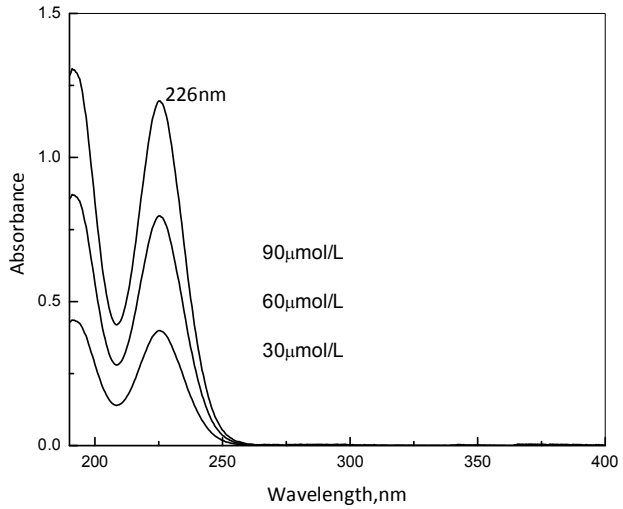

Figure A.2 Absorption spectrum of iodide in water

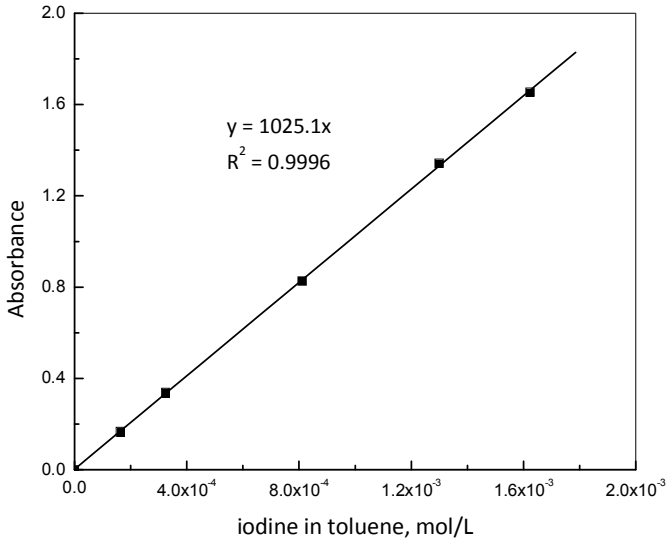

Figure A.3 UV calibration curve for iodine in toluene

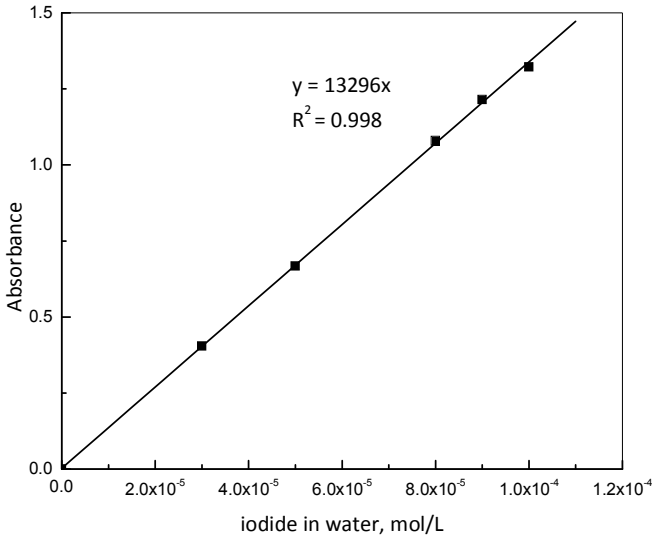

Figure A.4 UV calibration curve for iodide in water

APPENDIX B
Experimental Raw data

The reading for the pressure for each experiment is through the pressure transducer in which the unit of the pressure is in psi. Since the transducer read the pressure for every second, the tables with experimental raw data presented in this appendix only shows the first 60 seconds for the experiments in the group of different agitation speed to save space, other data can be found in the CD handed to Dr. Wang.

Table B.1 Raw data of pressure recorded for the runs of different agitation speed

Time	Pressure (psi)			
s	0 rpm	100 rpm	200 rpm	300 rpm
0	12.67	12.58	12.41	12.62
1	11.99	11.88	11.65	12.01
2	11.40	11.37	10.66	10.75
3	11.18	10.64	10.24	10.27
4	10.73	10.44	9.52	9.36
5	10.46	9.97	9.19	8.88
6	9.90	9.69	8.61	8.36
7	9.69	9.30	8.12	7.81
8	9.40	8.93	7.79	7.60
9	9.11	8.59	7.46	7.12
10	8.88	8.30	7.13	6.96
11	8.66	8.14	6.82	6.55
12	8.50	7.88	6.55	6.31
13	8.30	7.71	6.35	6.09
14	8.12	7.46	6.12	5.84

15	7.93	7.26	5.96	5.78
16	7.78	7.07	5.74	5.56
17	7.65	6.91	5.70	5.44
18	7.53	6.79	5.49	5.22
19	7.45	6.63	5.39	5.13
20	7.32	6.58	5.21	5.03
21	7.20	6.40	5.14	4.89
22	7.13	6.30	5.06	4.78
23	7.00	6.21	4.90	4.68
24	6.94	6.07	4.84	4.66
25	6.85	6.00	4.76	4.56
26	6.79	5.88	4.72	4.50
27	6.65	5.87	4.61	4.43
28	6.63	5.73	4.54	4.34
29	6.53	5.67	4.46	4.29
30	6.46	5.58	4.40	4.23
31	6.42	5.52	4.38	4.18
32	6.31	5.46	4.29	4.14
33	6.26	5.37	4.24	4.08
34	6.19	5.32	4.19	4.04
35	6.13	5.25	4.13	4.00
36	6.09	5.22	4.10	3.95
37	6.04	5.16	4.04	3.91
38	6.00	5.11	4.00	3.89
39	5.94	5.07	3.95	3.86
40	5.86	5.01	3.94	3.80
41	5.80	4.99	3.90	3.79
42	5.79	4.93	3.87	3.73
43	5.72	4.88	3.81	3.72
44	5.69	4.84	3.79	3.67
45	5.68	4.80	3.77	3.69
46	5.60	4.74	3.73	3.63

47	5.61	4.70	3.70	3.62
48	5.52	4.67	3.66	3.58
49	5.49	4.61	3.63	3.57
50	5.45	4.62	3.61	3.54
51	5.41	4.55	3.58	3.52
52	5.38	4.52	3.55	3.50
53	5.31	4.48	3.53	3.50
54	5.28	4.46	3.52	3.49
55	5.25	4.42	3.49	3.45
56	5.24	4.37	3.49	3.44
57	5.19	4.37	3.46	3.43
58	5.16	4.32	3.44	3.41
59	5.13	4.29	3.42	3.41
60	5.07	4.27	3.41	3.40

Besides, the analysis of the substances in both aqueous phase and toluene phase after each run of the experiment was conducted. Then mass balance with respect to the ion of iodine (Table 4.3) was carried out based on the data of the analysis. Table C.2 shows the analysis data of the runs after the experiments in the group of different iodine concentration at 22 ^{o}C to save space, other data can also be found in the CD handed to Dr. Wang.

Table B.2 Amount of various components after reaction with different $[I_2]$
SO_2 initial partial pressure: 79.2 kPa; phase ratio: 0.7:80; Agitation: 200 rpm

$[I_2]$ in toluene mol/L	I_2 left toluene mol	I_2 left water mol	I^- water mol	H^+ water mol
0.195	0.00199	0.00099	0.02498	0.05084
0.146	0	0	0.02263	0.04672
0.118	0	0	0.01843	0.03880
0.078	0	0	0.01227	0.02534
0.045	0	0	0.00692	0.01477